The Effects of Global Change upon United States Air Quality

R. Gonzalez-Abraham[1*], J. Avise[1,2], S. H. Chung[1], B. Lamb[1], E. P. Salathé, Jr[3], C. G. Nolte[4], D. Loughlin[4], A. Guenther[5**], C. Wiedinmyer[5], T. Duhl[5], Y. Zhang[5], D. G. Streets[6]

1. Washington State University, Pullman, Washington, USA
** Now at the Molina Center for Strategic Studies in Energy and the Environment, La Jolla, California, USA*
2. *California Air Resources Board, Sacramento, California, USA*
3. *University of Washington, Seattle, Washington, USA*
4. *Environmental Protection Agency, Research Triangle Park, North Carolina, USA*
5. *National Center for Atmospheric Research, Boulder, Colorado, USA*
** Now at Pacific Northwest National Laboratory, Richland, Washington, USA
6. *Argonne National Laboratory, Argonne, Illinois, USA*

Correspondence to R. Gonzalez-Abraham (rodrigoga@mce2.org)

Abstract

To understand more fully the effects of global changes on ambient concentrations of ozone and particulate matter with aerodynamic diameter smaller than 2.5 μm ($PM_{2.5}$) in the US, we conducted a comprehensive modeling effort to evaluate explicitly the effects of changes in climate, biogenic emissions, land use, and global/regional anthropogenic emissions on ozone and $PM_{2.5}$ concentrations and composition. Results from the ECHAM5 global climate model driven with the A1B emission scenario from the Intergovernmental Panel on Climate Change (IPCC) were downscaled using the Weather Research and Forecasting (WRF) model to provide regional meteorological fields. We developed air quality simulations using the Community Multiscale Air Quality Model (CMAQ) chemical transport model for two nested domains with 220 km and 36 km horizontal grid cell resolution for a semi-hemispheric domain and a continental United States (US) domain, respectively. The semi-hemispheric domain was used to evaluate the impact of projected Asian emissions changes on US air quality. WRF meteorological fields were used to calculate current (2000s) and future (2050s) biogenic emissions using the Model of Emissions of Gases and Aerosols from Nature (MEGAN). For the semi-hemispheric domain CMAQ simulations, present-day global emissions inventories were used and projected to the 2050s based on the IPCC A1B scenario. Regional anthropogenic emissions were obtained from the US Environmental Protection Agency National Emission Inventory 2002 (EPA NEI2002) and projected to the future using the MARKet ALlocation (MARKAL) energy system model assuming a business as usual scenario that extends

current decade emission regulations through 2050. Our results suggest that daily maximum 8 hour average ozone (DM8O) concentrations will increase in a range between 2 to 12 ppb across most of the continental US, with the highest increase in the South, Central, and Midwest regions of the US, due to increases in temperature, enhanced biogenic emissions, and changes in land use. The effects of these factors are only partially offset by reductions in DM8O associated with decreasing US anthropogenic emissions. Increases in $PM_{2.5}$ levels between 2 and 4 μg m^{-3} in the Northeast, Southeast, and South regions are mostly a result of enhanced biogenic emissions and land use changes. Little change in $PM_{2.5}$ in the Central, Northwest, and Southwest regions was found, even when PM precursors are reduced with regulatory curtailment. Changes in temperature, relative humidity, and boundary conditions shift the composition but do not alter overall $PM_{2.5}$ mass concentrations.

1. Introduction

Despite extensive efforts to reduce anthropogenic emissions, air pollution continues to be a public health issue in the United States (EPA, 2010). Elevated concentrations of pollutants in the troposphere, such as ozone (O_3) and particulate matter (PM), degrade air quality and have been associated with, among other things, increasing human respiratory diseases in urban areas (WHO, 2005) and low birth weights across the world (Dadvand et al., 2012).

High concentrations of tropospheric ozone and particulate matter with aerodynamic diameter smaller than 2.5 μm ($PM_{2.5}$) are caused by a combination of adverse meteorological conditions and the atmospheric emissions of their primary precursors. While regulatory controls are expected to reduce emissions of many pollutants in the United States (US) in the future, the negative effects of global climate change may offset the positive effects of such reductions. Furthermore, global emissions of greenhouse gases and other pollutant precursors are projected to increase (IPCC, 2007). Moreover, recent research has provided evidence of increasing long-range transport of ozone and $PM_{2.5}$ precursors from Asia and their influence over the western US. (Lelieveld and Dentener, 2000; Wuebbles et al., 2007; Zhang et al., 2010; Ambrose et al., 2011; WMO, 2012).

In the United States, regulations and technological changes in the transportation and energy sectors are projected to reduce regional atmospheric pollutants in the future (Loughlin et al., 2011). However, the interplay between climate change, increasing

global emissions, and intercontinental transport pose challenges that air quality managers will have to address in order to maintain regional air quality standards (Ravishankara et al., 2012). To provide a foundation for building effective management strategies and public policies in a changing global environment, modeling approaches that link global changes with regional air quality are required. The general approach has been to use output from general circulation models (GCMs) to drive regional climate models (RCMs) and regional or global chemical transport models (CTMs/GTMs; Giorgi and Meleux, 2007; Jacob and Winner, 2009).

This downscaling approach has been used in a variety of studies in Europe, Canada, and Asia (e.g., Liao et al., 2006; Langner et al., 2005; Forkel and Knoche, 2006; Meleux et al., 2007; Kunkel et al., 2007; Lin et al., 2008; Spracklen et al., 2009; Kelly et al., 2012). These investigations based the global emissions on future anthropogenic emissions scenarios developed from the Intergovernmental Panel on Climate Change (IPCC) assessment reports. Despite the differences in emission scenarios, modeling framework and future climate realizations, increases in ozone concentrations on the order of 2 to 10 ppb were consistently predicted from these studies as a result of climate change alone. By contrast, there is little consistency among the model predictions of climate change effects on particulate matter (PM) (Jacob et al, 2009; Dawson et al., 2013).

In the US, a combined effort between the EPA and the academic community resulted in a set of modeling studies that adopted a variety of modeling methods (Hogrefe et al., 2004; Leung and Gustafson, 2005; Liang et al., 2006; Steiner et al.,

2006; Tagaris et al., 2007; Liao et al., 2006 Tao et al., 2007; Huang et al., 2007, 2008; Nolte et al., 2008; Wu et al, 2008a, 2008b; Chen et al, 2009b; Avise et al., 2009). These US investigations based their current and future climate realizations on the results of GCMs using the various IPCC emissions scenarios (IPCC, 2007). In some of the studies, the global climate realizations were subsequently downscaled to a higher resolution using the PSU (Pennsylvania State University)/NCAR (National Center for Atmospheric Research) Mesoscale Model version 5 (MM5; Grell et al., 1994) to horizontal resolutions that ranged from 90 km to 36 km. Many of these studies based their analysis on the effects of climate change on summer air quality in the Continental US (CONUS). In summary, despite the differences in modeling elements, all studies found an increase in daily maximum summer ozone concentrations on the order of 2 to 8 ppb for the simulated CONUS domain (Weaver et al., 2009), but with regional variations. In contrast, PM concentrations showed changes between ± 0.1μg m^{-3} to ± 1μg m^{-3}, with little consistency between studies, including the sign of the differences (Jacob and Winner, 2009).

It is important to note that variations between modeling frameworks did result in very diverse regional patterns of key weather drivers for ozone and PM formation. Thus, while most of the studies mentioned above found an average increase in ozone concentrations for the simulated domains, reductions or insignificant changes in certain regions of the domain were also simulated. Generally, temperature and solar radiation reaching the surface were the major meteorological drivers for regional ozone concentrations. For PM concentrations, most of the studies found a direct link between

118 changes in precipitation and relative humidity and changes in PM concentrations (Liao
119 et al., 2006; Unger et al., 2006; Racherla and Adams 2006, Tagaris et al., 2007; Avise
120 et al., 2009; Chen et al., 2009b). Nevertheless, the direct impacts of changes in
121 meteorological conditions are not the only factors of change for ozone and PM
122 concentrations. Changes in emissions of biogenic volatile organic compounds (BVOCs),
123 due to climate and landcover change, and the treatment of isoprene nitrates in the
124 chemical mechanism were found to be a key factor in the regional variability of ozone
125 and PM, particularly in areas of the southeastern US (Jacob and Winner, 2009; Weaver
126 et al., 2009).

127 In this work, we present a continuation of the work described by Avise et al.
128 (2009) and Chen et al. (2009a,b), who downscaled the Parallel Climate Model (PCM;
129 Washington et al., 2000) and MOZART (Model for OZone And Related chemical
130 Tracers; Horowitz, 2006) global model output for the A2 IPCC scenario using MM5 and
131 the Community Multi-scale Air Quality Model (CMAQ; Byun and Schere, 2006) to
132 simulate current and future air quality in the US. For this update, we implemented a
133 semi-hemispheric domain for the Weather Research and Forecasting (WRF) mesoscale
134 meteorological model (http://www.wrf-model.org) and CMAQ simulations in lieu of using
135 MOZART output for chemical boundary conditions for our CONUS CMAQ simulations.
136 We used the ECHAM5 global climate model (Roeckner et al., 1999, 2003) output for the
137 A1B scenario to drive these simulations for two decadal periods; the current decade
138 from 1995–2004 and the future decade 2045–2054. In presenting our results, we follow
139 the attribution approach described in Avise et al. (2009), where the separate and

combined effects of changes in climate, US anthropogenic emissions, global anthropogenic emissions and biogenic emissions due to changes in regional meteorology and land use are investigated. Ideally, this framework should include feedback from changes in atmospheric chemistry to the climate system (Raes et al., 2010). However, due to the computational requirements of an on-line approach, we did not incorporate feedback between the atmospheric chemistry and transport simulations from the CTM to the RCM. Furthermore, despite the observed sensitivity of tropospheric ozone to regional emissions and global burden of methane (Zhang et al., 2011; Fiore et al., 2008; Wu et al., 2008a; Nolte et al., 2008; Fiore et al., 2006), in this work, we do not address the potential contribution of methane.

In Section 2, we provide an overview of the modeling framework and emissions scenarios. Evaluation of the model performance for the climate simulations and results of the changes in meteorological fields are presented in Section 3. Assessment of air quality changes and the individual and combined effects from changes in model components are presented in Section 4. Finally, we present a summary of the results and conclusions in Section 5.

2. Methodology

2.1 General Framework

Results from the global climate model ECHAM5 under the IPCC Special Report on Emissions Scenarios (SRES) A1B scenario (Nakicenovic et al., 2000) were downscaled using the WRF model separately to a semi-hemisperic (S-HEM) 220 km

domain and nested CONUS domains of 108 km (not shown) and 36 km (Figure 1). Due to computational limitations, only five representative summers for the present (1995 to 2004) and the future (2045 to 2054) decades were selected. Ranked in terms of their average maximum temperature of the year, the summers of the warmest and coldest years, as well as the second, fifth and seventh warmest years in each decade were treated to represent the present and future climate conditions for each decade. These five representative summers (June-July-August; with May as a spin-up period) for the present and future periods were processed with the Meteorology-Chemistry Interface Processor v3.4.1 (MCIP; Otte and Pleim, 2010) for the S-HEM and 36 km CONUS domains. Meteorological fields generated from MCIP for both domains were used to estimate biogenic emissions using the Model of Emissions of Gases and Aerosols from Nature v2.04 (MEGANv2.04; Guenther et al., 2006) and to calculate the temporal profiles within the Sparse Matrix Operator Kernel Emissions (SMOKE) v2.7 (http://www.smoke-model.org). With the elements described above, a framework to perform air quality simulations using the Community Multiscale Air Quality Model (CMAQ v4.7; Foley et al., 2010) was created. The overall schematic for the modeling system is shown in Figure 2.

2.2 Climate and Meteorology

The regional weather model WRF includes advanced representations of land-surface dynamics and cloud microphysics to simulate complex interactions between atmospheric processes and the land surface characteristics. Detailed descriptions of WRF can be found at http://wrf-model.org and a discussion of its range of regional

climate modeling applications can be found in Leung et al. (2006). In this experiment, WRF was used to downscale the ECHAM5 output for both the S-HEM and 108/36 km CONUS domains. The model was applied with 31 vertical levels and a vertical resolution of ~ 40 – 100 m throughout the boundary layer with the model top fixed at 50 mb. Details of the model setup and a discussion of the results are reported by Salathé et al. (2010), Zhang et al. (2009, 2012), and Duliére (2011, 2013).

2.3 Current and Future Biogenic Emissions and Land Use Changes

The MEGANv2.04 biogenic emission model (Guenther et al., 2006, Sakulyanontvittaya et al., 2008) was used to estimate current and future biogenic VOC and soil NO_X emissions based on the WRF meteorology with current and future estimates of land use and land cover. For the current decade, the default MEGANv2.04 land cover and emission factor data (Guenther et al., 2012) were used. For the future decade, cropland distributions were estimated by combining three datasets: the IMAGE 2100 global cropland extent dataset, (Zuidema et al., 1994), the SAGE maximum cultivable land dataset (Ramankutty et al., 2002), and the MODIS-derived current cropland data (as used in MEGANv2 and described in Guenther et al., 2006). The IMAGE 2100 dataset was created from the output of a land cover model, which forms part of a sub-system of the IMAGE 2.0 model of global climate change (Alcamo, 1994). The SAGE cultivable dataset was created using a 1992 global cropland dataset (Ramankutty and Foley, 1998) modified by characterizing limitations to crop growth based on both climatic and soil properties. The future global cropland extent distribution was generated by analyzing predicted changes in agriculture on a continent-by-continent basis (using the

IMAGE data). These changes were then applied to the MODIS based cropland map (used for present day MEGAN simulations) using the SAGE maximum cultivable dataset as an upper limit to cropland extent. The resulting landcover data has considerably lower cropland fraction than the original IMAGE data, which likely overestimates future cropland area by not considering whether a location is cultivable.

In addition to generating a future crop cover dataset to simulate potential biogenic VOC emissions using MEGAN, future datasets representing several other MEGAN driving variables were developed. These included geo-gridded potential future plant functional type (PFT)-specific emission factor (EF) maps for isoprene and terpene compounds, as well as future-extent maps of four non-crop PFTs: broadleaf trees, needle-leaf trees, shrubs, and grasses. For regions outside of the US, the non-crop PFT distributions were generated by reducing the current extent of each non-crop PFT map by an amount that would appropriately offset the predicted cropland expansion for a given continent. For the US, future non-crop PFT maps were generated using the Mapped Atmosphere-Plant-Soil System (MAPSS) model output (http://www.fs.fed.us/pnw/corvallis/mdr/mapss/; Neilson, 1995), based on three GCM future scenarios. Present-day MAPSS physiognomic vegetation classes were associated with current PFT fractional coverage estimates by dividing the US into sub-regions and by averaging existing (MODIS-derived) geospatially explicit PFT data within each sub-region as a function of MAPSS class. Sub-regions were created based on Ecological Regions of North America (http://www.epa.gov/wed/pages/ecoregions.htm). After every current MAPSS class had been assigned PFT-specific fractional coverage

227 estimates, future PFT cover was determined by re-classifying future distribution maps
228 for the three MAPSS datasets using the fractional PFT cover estimates for each
229 MAPSS class (within each ecological region), and averaging the three resultant future
230 datasets into a single estimate of future cover for each PFT.

231 For the eastern US, future isoprene and monoterpene PFT-specific EF maps
232 were constructed using changes in tree species composition predicted by the USDA
233 'Climate Change Tree Atlas' (CCTA, http://nrs.fs.fed.us/atlas/tree/). The CCTA data was
234 based on the average of three GCMs, which represented the most conservative
235 emissions scenarios available.

236 Using existing speciated EF data (Guenther, 2013), we applied anticipated
237 changes in the average species composition of each PFT to generate species-weighted
238 PFT-specific EF maps on a state-by-state basis (the CCTA data is organized by state).
239 As data was lacking on predicted species-level changes for areas outside the eastern
240 US, we did not attempt to alter EF maps outside the eastern US.

241 **2.4 Anthropogenic Emissions**

242 For S-HEM domain CMAQ simulations, global emissions of ozone precursors
243 from anthropogenic, natural, and biomass burning sources were estimated for the
244 period 1990-2000 (applied to 1995-2004) using the POET emission inventory (Granier
245 et al., 2005). Non-US anthropogenic emissions (containing 15 sectors) were projected
246 based on national activity data and emission factors. Gridded maps (e.g. population
247 maps) were applied to spatially distribute the emissions within a country. The global

emission inventory for black and organic carbon (BC and OC respectively) was obtained from Bond et al. (2004), which uses emission factors on the basis of fuel type and economic sectors alone. The Bond et al. (2004) inventory includes emissions from fossil fuels, biofuels, open burning of biomass, and urban waste. Considering combinations of fuel, combustion type, and emission controls, as well as their prevalence on a regional basis covers the dependence of emissions on combustion practices.

Global emissions for the year 2000 from the POET, MEGAN, and Bond et al. (2004) inventories were combined, and the 16 gas-phase POET and MEGAN species, along with the OC and BC species were adapted to the SAPRC99 (Carter 1990, 2000) chemical mechanism. Diurnal patterns were developed and applied to the gridded emission inventories and processed using SMOKE. For the future decade hemispheric domain simulations, current decade emissions were projected to the year 2050 based on the IPCC A1B emission scenario.

For the 36-km CONUS current decade CMAQ simulations, US anthropogenic emissions were developed using the 2002 National Emission Inventory. The Emission Scenario Projection (ESP) methodology, version 1.0 (Loughlin et al., 2011), was applied to project future decade US anthropogenic emissions. A primary component of ESP 1.0 is the MARKet Allocation (MARKAL) energy system model (Loulou et al., 2004). MARKAL is an energy system optimization model that characterizes scenarios of the evolution of an energy system over time. In this context, the energy system extends from obtaining primary energy sources, through their transformation to useful forms, to the variety of technologies (e.g., classes of light-duty personal vehicles, heat pumps, or

gas furnaces) that meet “end-use” energy demands (e.g., projected vehicle miles traveled, space heating). Within ESP 1.0, the MARKAL is used to develop multiplicative factors that grow energy-related emissions from a base year to a future year. Surrogates, such as projected population growth or industrial growth, are used to develop non-energy-related growth factors. The resulting factors were used within SMOKE to develop a future decade inventory from the 2002 NEI inventory.

For the work presented here, the EPAUS9r06v1.3 database (Shay et al., 2006) was used with MARKAL to develop growth factors for NOx, SO_2 and PM_{10}. The PM_{10} growth factors were also applied to $PM_{2.5}$ and the CO_2 factors were used as a surrogate for energy system CO, NH_3, VOC, HCl and chlorine. Non-combustion industrial emission growth factors were developed from projections of economic growth. The resulting energy and non-energy factors were then used within SMOKE to multiply emissions from the 2002 National Emissions Inventory (NEI) to 2050.

EPAUS9r06v1.3 originally was calibrated to mimic the fuel use projections of the U.S. Energy Information Administration’s 2006 Annual Energy Outlook (AEO06; U.S. DOE, 2008). Energy demands were adjusted to account for population growth consistent with the A1B storyline. The results reflect business as usual assumptions about future environmental and energy regulations as of 2006. Thus, while electric sector emissions are capped to capture the effects of the Clean Air Interstate Rule (CAIR; US EPA, 2005), the impacts of increases in natural gas availability, the recent economic downturn, and the relatively new 54.5 Corporate Average Vehicle Efficiency (CAFÉ) standard (US CFR, 2011) are not reflected. More recent versions of the

292 MARKAL database reflect these factors, expanded pollutant coverage, and refined
293 emission factors (U.S. EPA, 2013). The ESP 1.0, including the MARKAL database
294 EPAUS9rv1.3 was selected here to maintain compatibility with previous and ongoing
295 activities.

296 After SMOKE was used to develop a 2050 inventory, the differences between the
297 base year and future-year inventories were summarized at the pollutant and regional
298 level, as shown in Figure 3. Using the ESP1.0 methodology, emissions of NO_X and SO_2
299 are projected to decrease between 16% in the South and Southwest to 35% in the
300 Northeast and Northwest. On the other hand, emissions of pollutants that were not
301 captured endogenously in MARKAL, such as carbon monoxide (CO), volatile organic
302 compounds (excluding methane; NMVOCs) and ammonia (NH_3) are projected to
303 increase in nearly all regions across the CONUS domain. The largest increase of CO is
304 projected in the Midwest with a 70% increase combined with an increase of about 20%
305 of NMVOC. The smallest increase of CO is projected for the South; however, the same
306 region was projected to increase NMVOC by about 12%. The smallest increase (3%) of
307 PM is projected in the central region, which also has a 34% increase in NMVOC.

308 **2.5 Air Quality Simulations**

309 The CMAQ model version 4.7.1 was employed to simulate the potential impact of
310 climate change on surface ozone and $PM_{2.5}$ over the CONUS at 36 km horizontal grid
311 spacing and covering 18 vertical layers from the surface up to 100 mb. The model
312 configuration included the use of the SAPRC99 chemical mechanism and version 5 of
313 the aerosol module.

Using the framework components described above, a matrix of CMAQ simulations that included changes in predicted meteorological conditions and potential emission scenarios was constructed (Table 1). For each set of simulations shown in Table 1, five representative summers were modeled. Simulation 0 represents the base case simulation, where all model inputs are set to current decade conditions. Simulation 1 is used to investigate the impact of climate change alone; where all model inputs are set to current decade conditions except for meteorology (biogenic emissions are not allowed to change with the future climate for this case). Simulation 2 is the same as Simulation 1, except that biogenic emissions are allowed to change with the future climate, and in Simulation 3 future land use is also incorporated into the biogenic emission estimates. Simulation 4 is used to investigate the impact of future decade US anthropogenic emissions, where all inputs are set to current decade levels except for US anthropogenic emissions. The impact of future global emissions is investigated in Simulation 5, and Simulation 6 represents the combined impacts of Simulations 1-5.

2.6 Evaluation of Model Performance

To aid in summarizing model results, the 36 km domain was divided geographically into 7 regions (Figure 3, lower right). Since the WRF simulations used to drive CMAQ are based on a climate realization rather than reanalysis data, a direct comparison between the modeled output and observations cannot be made. Instead, the frequency distributions of simulated and observed values are compared. For the simulated meteorological fields, daily maximum temperature, and daily precipitation are compared against a decade of summer observations (1995 to 2004) from the United

States Historical Climatological Network (US-HCN; http://cdiac.ornl.gov/ftp/ushcn_daily/; Karl et al., 1990) in Figure 4. The model distributions of temperature and precipitation agree reasonably well with the observations, and provide a good representation of the regional variability of precipitation and temperature. Except for the Northwest and Southwest regions, the observed mean and maximum temperatures are slightly over predicted. However, for all analyzed regions the model successfully simulates the seasonal trend of summer temperatures, showing the observed increase in mean temperature from June to July and subsequent decrease in mean temperature from July to August (not shown).

The modeled daily maximum 8 hr ozone concentrations (DM8O) from the five representative summers (Figure 5) from the current decade CMAQ simulations (Simulation 0 in Table 1) were compared to the range of observations from the AIRNow network (http://airnow.gov/). As seen in Figure 5, DM8O tends to be over-estimated in regions where temperature maxima is also over predicted, such as the South, Midwest, Southeast and Northeast. Except for the less populated Central region, DM8O shows a bias that ranges between +10 ppb (+15%) and +25 ppb (+37%) across the domain. This is consistent with previous climate downscaled results by Tagaris et al. (2007), who found a bias of +15% and with Avise et al. (2009) who found regional biases as high as +39%. Despite the bias, results from the modeling framework presented here have been shown to accurately represent the correlation between ozone and temperature at rural CASTNET sites throughout the US (Avise et al., 2012).

Simulations for the current decade show a mean DM8O of 66 ± 20 ppb (standard deviation between simulated DM8O for the five summers), while the observed average at the AIRNow sites was 53 ± 19 ppb. Simulations successfully captured the enhanced DM8O concentrations over the major urban areas and regions with high biogenic sources (Figure 10, top). Variability of the simulated DM8O concentrations between summers is on the order of 10% (not shown) in highly populated areas and down to 1% in less populated areas, with the greatest variability found in the Northeast region.

Simulated concentrations of current decade $PM_{2.5}$ ($PM_{2.5}$ with no water content, unless otherwise specified) show a five summer average of 5.6 ± 0.7 μg m^{-3}, compared to 14.3 ± 9.2 μg m^{-3} observed at the Speciation Trends Network (STN; US EPA, 2000). Simulated $PM_{2.5}$ show the highest concentrations occurring inland of coastal regions and throughout the Northeast and Southeast (Figure 11, top).

In general, the model underestimates the concentrations of $PM_{2.5}$ across most regions by between 25% in the Midwest to more than 50% in the Central region. Underestimation of $PM_{2.5}$ in CMAQ has been documented as a result of several factors including an underprediction of SO_4^{2-}, a lack of windblown dust emissions, and an underestimation of Secondary Organic Aerosol (SOA) formation (Carlton et al., 2010; Foley et al., 2010; Appel et al., 2012; Luo et al., 2011). In our study, when comparing to the STN data, we found an underestimation of all species, including SO_4^{2-} and total carbon (Organic Carbon + Elemental [Black] Carbon), except for the un-speciated $PM_{2.5}$ species (also known as PM “other"). Nevertheless, when comparing the average fractional composition we found a slight overestimation of the SO_4^{2-} fraction for most

regions (Figure 6, top panel). Most regions were also found to underestimate the NO_3^- and NH_4^+ fractions. Low concentrations of NH_4^+ relative to SO_4^{2-} result in a sulfate-rich system, where aerosols are dominated by aqueous phase HSO_4^- and SO_4^{2-} and have lower concentrations of $(NH_4)_2SO_4$ and NH_4NO_3 (Fountoukis and Nenes, 2007; Kim et al., 1993; Sienfield and Pandis, 2006). Further discussion of the response of the inorganic aerosol system to global changes is provided in Section 3.4.

When compared to STN data (Figure 6, top panel), we found a large underestimation of the fraction of organic carbon in all regions, while the unspecified fraction was over-predicted. The unspecified fraction in CMAQ is composed of all the non-carbon atoms associated with the OC fraction, unspecified direct $PM_{2.5}$ emissions, and other trace species (Foley et al., 2010). The underprediction in OC reflects the uncertainties in precursor sources and the SOA formation mechanisms which have been previously documented (e.g., Carlton et al., 2010; Foley et al., 2010).

Speciated $PM_{2.5}$ model performance using mean fractional error (MFE) and mean fractional bias (MFB) statistics for the major $PM_{2.5}$ components as suggested by Boylan and Russell (2006) was performed (Figure 6, middle and bottom panels). The majority of the speciated components show MFE and MFB within the criteria threshold for most regions. Furthermore, the model performance was within these guidelines for $PM_{2.5}$ in four of the seven regions, and only in the Central region did the model not meet these guidelines. Similarly, SO_4^{2-}, NO_3^-, NH_4^+ and unspecified fractions meet the benchmark thresholds for model performance in most regions. In terms of the unspecified fraction, the better model performance in most regions is due to the heavy contribution to the

total mass of the $PM_{2.5}$. For the SO_4^{2-}-NO_3^--NH_4^+ system, the values for the MFE and MFB indicate that the model performed sufficiently well in responding to the conditions that drive inorganic aerosol formation. These values increase the confidence about the response to global changes in the system. In the case of OC and EC, poor model performance was found, with concentrations largely underpredicted for all regions.

3. Results and Discussion

3.1 Projected Changes in Meteorology

Projected changes in selected meteorological parameters are shown in Figure 7. Except for some minor cooling along the Pacific coast, mean summer temperature across the continental US is projected to increase between 0.5 and 4°C (Figure 7a). This increase falls within the lower bound of the warming predicted by the ensemble of 20 GCM's under the A1B emission scenario described by Christensen et al., (2007), but differs in the regional variability due to the higher resolution of our simulations. When compared to similar studies of equal resolution using a GCM (e.g. Goddard Institute for Space Studies, GISS II) driven by the A1B IPCC emission scenario and downscaled with MM5 to 36-km resolution, our simulated temperatures show higher temperature differences between future and current decades (Leung and Gustafson, 2005; Tagaris et al., 2007). Furthermore, Tagaris et al. (2007) and Leung and Gustafson (2005) predicted an average increase between 1 and 3 ^{o}C for most of the domain, and temperature reductions in the border states of the Central and South regions. Nevertheless, despite the differences in physical parameterizations contained in the GCMs and the driving IPCC emission scenarios that were used, similar temperature

differences (2 to 4 ^{o}C) between our study and previous investigations were simulated for the Northeast and Southeast regions (Leung and Gustaffson, 2005; Tagaris et al., 2007; Avise et al., 2009).

Projected changes in precipitation across the US vary depending on the region. With the exception of the Northwest and the northern boundary of the Central region, summertime precipitation is projected to decrease between -10% and -80%. The largest decrease is projected in the Southwest region. Our results show greater precipitation reductions than those presented in Christensen et al., (2007) who predicted between a -5 to -15% decreases in the South and Southwest regions. Also, previous investigations agreed with our predicted mean precipitation reductions across the domain (Figure 7c). In the Northwest, the modeled increase in precipitation is also consistent with Leung and Gustafson (2005), who projected an increase in precipitation throughout the Northwest region. In contrast, the Southeast and Northeast regions show disparities in the magnitude and the sign of the change in precipitation. While our simulations predict a reduction in precipitation between -10 to -20%, the ensemble of 20 GCM's predicted an increase between 5 to 10% across the same regions. The disparity may be a result of the differences in resolution and parameterization schemes between our study and those used for the 20 GCM's.

Projected increases in solar radiation reaching the ground also vary by region. A decrease in solar radiation in the Northwest that extends to the northern boundaries of the Central regions is simulated. Small changes in the Southwest, South and Midwest are also predicted, with the largest increase experienced in the Northeast and

Southeast regions (Figure 7b). Similar results for the Northeast regions are reported for previous investigations (Leung and Gustafson, 2005; Tagaris et al., 2007, and Avise et al., 2009). However, these same investigations had higher reductions at the border between the Central and South regions.

Changes in relative humidity are shown in Figure 7d. Relative humidity is predicted to decrease in most of the domain except for the regions where decreases in solar radiation were projected. The greater decrease in relative humidity occurs in the Southwest and Central regions of the domain, and the largest increase is observed in the Northwest region.

3.2 Changes in Biogenic Emissions

The only region that is projected to have reduced total BVOC emissions is the Northwest, where, despite the increase in monoterpenes, a 7% reduction in isoprene (Figure 3) is simulated. The reduction in isoprene emissions is a result of the decrease in temperatures in areas where the higher emissions are encountered (Figure 7).

Furthermore, despite having the biggest increase in monoterpenes in the Central and South regions, the larger increase in isoprene for the Midwest, followed by the Northeast, Southeast, South, Central and Southwest regions, drives the increase in total BVOC. The increase in BVOC ranges between 17% and 45%. Previous investigations (Liao et al., 2006, Nolte et al., 2008) show the greatest increase in BVOC emissions in the Southeast region (10-50%). Similarly, Leung and Gustafson (2005) predicted the

465 greatest increase in BVOC in the Southeast, but did not show any significant changes in
466 the Northwest region.

467 Average summertime isoprene emissions over five summers of simulation for
468 each decade are shown in Figure 8a. As expected, isoprene emissions occur at
469 relatively high rates (>50 metric tons/day) in the eastern US and at much lower rates in
470 the western US (<10 metric tons/day). When the emissions are projected to future
471 climate conditions with current land use distributions, isoprene emissions are projected
472 to increase across the domain (average increase of about 30%; Figure 8b) with the
473 most noticeable increases occurring in the Northeast and Southeast regions. However,
474 when future climate is combined with future land use, there are still increases in the
475 eastern US, but the spatial extent of the increase is reduced, reflecting the expansion of
476 low isoprene-emitting croplands into regions of high isoprene-emitting deciduous
477 forests. In this case, the domain-average increase was approximately 12% of current
478 decade emissions, compared with a 25% increase when changes in land use are not
479 included (Figure 9a). Thus, future expansion of cropland and subsequent reduction of
480 broadleaf forested lands are projected to lessen the overall increase in US isoprene
481 emissions that result from a warmer climate. Future monoterpene emission estimates
482 increase because of higher across the domain. Since the version of MEGAN used in
483 this work does not include the suppression of isoprene emissions due to elevated
484 concentrations of CO_2 (Rosenstiel et al., 2003; Heald et al., 2009), the future estimates
485 in this study are likely to be an upper bound on isoprene emissions, and it is likely that
486 future isoprene emissions will be lower than predicted by this work. Monoterpene

emissions from US landscapes are not expected to be suppressed by increasing CO_2 and so are not impacted by omitting this process.

When the future decade meteorology is combined with future land use (Figure 9b), an increase of over 100% of current decade monoterpene emissions is predicted. The growth is most noticeable in the Central, South and Midwest regions. Also, an overall increase between 25% and 50% for the Western and Eastern regions is predicted. This limited increase is primarily driven by the projected changes in land use predicted for those regions.

3.3 Effects of Global Changes upon Ozone Concentrations

Results for how the various global changes affect DM8O are summarized in Table 2 and Figure 10. Simulations for the future decade (Simulation 6) show higher DM8O across the domain than the current decade simulation (Simulation 0) with a domain average of 51 ± 10 ppb. In general, increases in DM8O are due to growing global anthropogenic emissions and climate change, while decreasing US emissions reduce DM8O. Changes in biogenic emissions as a result of a changing climate and land use have less of an influence on DM8O; the influence can be either positive or negative depending on the region. These various factors are discussed in the following sections.

3.3.1 Contributions from Changes in Global and Regional Anthropogenic Emissions

The effects of increased long-range transport of emissions from Asia and Mexico are shown in Figure 10f. The changes in chemical boundary conditions (the difference

between Simulations 0 and 5 in Table 1) increase DM8O between 2 to 6 ppb across the CONUS domain. The general west-to-east gradient of the change in DM8O reflects intercontinental transport of ozone and its precursors from the west. The greatest impact is predicted in the South (6 ppb) and Southwest (4 ppb) regions. These results are consistent with Avise et al., (2009) who showed increases between 3 and 6 ppb of DM8O across the domain, with the greatest increase in the Southwest and South regions. The effects of future global emissions and intercontinental transport of ozone precursors in the continental US have also been investigated by Hogrefe et al. (2004), who predicted an increase of 5 ppb in the Northeast region under the A2 IPCC emission scenario.

Changes in regional US emissions of ozone precursors (difference between Simulations 0 and 4) reduce DM8O concentrations between 2 and 15 ppb across the domain. Larger reductions are observed in the Northeast (-15 ppb) and Southwest (-10 ppb) regions (Figure 10e). Similar results are shown in Nolte et al., (2008) and Tagaris et al., (2007) despite a difference in the magnitude of projected emissions reductions. Tagaris et al., (2007) simulated similar ozone reductions (about 9%), with a higher nationwide reduction of 51% in NO_X emissions and a slight increase (about 2%) in VOC emissions from A1B projections based on the Clean Air Interstate Rule (CAIR) emission inventory. Nolte et al., (2008) showed a decrease in ozone across the domain (-12 to -16 ppb) as a result of projected reductions of 45% for NO_X and 21% for VOC emissions from the NEI 2002, following the A1B IPCC emission scenario. In contrast, our future simulations included a 21% reduction in NO_X emissions and a slight increase (about

2%) in VOC emissions. Avise et al., (2009) predicted an average contribution of +3 ppb across the domain as a result of projecting the NEI 1999 (NEI-1999) with the Economic Growth Analysis System (EGAS) and the A2 IPCC emission scenario; increasing emissions by 5% for NO_X and 50% for VOCs in the future.

3.3.2 Contributions from Changes in Meteorological Fields

Figure 10d shows the difference between simulations that include changes in meteorological conditions (without the effect of biogenic emissions or land use) and the current decade base case (Simulations 0 and 1). The greater reductions in DM8O concentrations resulted from an increase in cloud cover, and a reduction in photochemistry due to lower solar radiation reaching the ground (Figure 10b), similar to the results of Jacob and Winner, 2009. Nevertheless, increases in DM8O concentrations were projected (+5 ppb) because increases in temperature had a greater impact on the ozone chemistry; this is particularly evident in the Midwest, Northeast and Southeast regions.

3.3.3 Contributions from Changes in Biogenic Emissions and Future Land Use

When biogenic emissions are allowed to change with the future meteorology, an average increase of DM8O with respect to the current decade base case simulations is predicted (Simulations 0 and 3). Increases of as much as 7 ppb in DM8O concentrations are mainly predicted in areas with substantial biogenic sources (Figure 10c). Similar results are shown by Leung and Gustafson (2005) and Tagaris et al. (2007), both predicted an increase of DM8O above 5 ppb in the east coast. Simulated reductions between 2 to 4 ppb of DM8O in the coastal areas of the western regions are probably due to cooler temperatures and increased cloud cover. Minor changes in

DM8O concentrations are shown over the Southwest and Northwest regions. This is in agreement with Avise et al. (2009) and Leung and Gustafson (2005) who predicted reductions in DM8O concentrations from 1 to 4 ppb in the western regions, while Tagaris et al. (2007) also predicted similar reductions in ozone in the Central and Midwest regions. The disparities between this investigation and Avise et al. (2009) are reasonable due to the different climate realizations used (A2 vs. A1B; Storyline in scenario A2 consider higher emissions of CO_2 by 2050 than the scenario A1B). However, the difference in geographical features of ozone changes with Leung and Gustafson (2005) and Tagaris et al. (2007) suggests that the source of disparities resides in both the climate realization and the methods used to estimate emissions from biogenic sources.

When the results from Simulation 2 are compared to the climate-only simulations (Simulation 1, Fig. 10b), our results suggest that changes in the meteorological fields are the main driver of DM8O enhancement in Simulations 2 and 3 (Fig. 10 c and d) across the domain. The change in biogenic emissions leads to an increase in the VOC to NO_X ratio relative to the climate-only (Simulation 1). This decrease between the Simulation 2 and Simulation 1 in our simulated DM8O suggests that the effect of sequestration of ozone precursors by the biogenic VOCs is predominant over the effect of recycling of isoprene nitrates considered in SAPRC99. A similar effect was reported by Xie, et al. (2012), who simulated an increase of 2 ppb of ozone when sequestration by isoprene nitrates was reduced in the chemical mechanism. Furthermore, when land use changes are included along with biogenic emissions (Simulation 3), the increase in

VOC to NO_X ratio is reduced and less depletion in DM8O is simulated, thus, higher concentrations of DM8O than the Simulation 2 are also observed. This lower VOC to NO_X ratio is due to the increase in soil NO associated with the land use change from natural vegetation to cropland.

3.3.4 Contributions from Combined Global Change to Future Changes in DM8O Concentrations

When the combined global changes are considered (Simulation 6), DM8O is projected to increase in nearly all regions except along the western and eastern coastlines and inland areas of those regions. Increases of DM8O between 4 to 12 ppb in the South, Central and Midwest regions are shown along with reductions of 4 ppb in parts of the Southwest and Northwest regions (Figure 10g). The increase in DM8O is mostly due to an increase in global emissions of ozone precursors from the semi-hemispheric domain (Figure 10f). The other contributing factors to increasing DM8O are a combination of changed meteorology (Figure 10b) and higher BVOC emissions (with current and future land use; Figure 10c,d). Reductions in DM8O in the urban areas resulted generally from reductions in ozone precursors from regional anthropogenic sources (Figure 10e). However, in the western regions, lower DM8O are the result of a combination of favorable meteorological conditions (e.g. reduction in temperature and solar radiation reaching the ground) and reductions in regional ozone precursors.

3.4 Effects of Global Changes upon $PM_{2.5}$ Concentrations

Results for how the various global changes affect $PM_{2.5}$ composition and concentrations are summarized in Tables 3-5 and Figure 11. Overall, reductions in US anthropogenic emissions have the largest impact on $PM_{2.5}$, with a reduction in

concentration in all regions. Changes in global emissions generally lead to increases in $PM_{2.5}$ in the western US, while changes in the climate and biogenic emissions can lead to both increases and decreases in $PM_{2.5}$ depending on the region.

3.4.1 Contribution to $PM_{2.5}$ Concentrations from Changes in Global and Regional Anthropogenic Emissions

Due to the relatively short atmospheric lifetime of PM, the effects from long-range transport and increasing Asian emissions on US $PM_{2.5}$ concentrations are relatively small in comparison to the current decade $PM_{2.5}$ concentrations (Figure 11f). Similar results are shown in Avise et al. (2009), who predicted a change of less than 1 μgm^{-3} as a result of changes in future chemical boundary conditions. However, when the chemical composition is analyzed, simulations show an increase in aerosol nitrate (NO_3^-) in the Northwest, South, and Southwest regions (Table 2) as a result of increased NO_X emissions from Asia and Mexico. In contrast, Avise et al. (2009) predicted no change in NO_3^- for the same regions. Furthermore, Avise et al. (2009) showed higher concentrations (by 7% to 25%) of SO_4^{2-} for the same regions resulting from higher global SO_2 emissions. Changes in global anthropogenic emissions cause reductions in SOA in the Southwest, Central, South, and Southeast regions and an increase in the Northwest, Midwest and Northeast Regions (Table 4). However, the simulated changes in SOA are very small and the variation is probably due to small differences in modeled OH radical concentrations.

In the US, reductions in regional SO_2 and NO_X emissions from regulatory curtailment result in a significant reduction of $PM_{2.5}$ in urban areas. The greatest decrease, between 4 to 6 $\mu g\ m^{-3}$, is found in the Midwest and Northeast regions (Figure

622 11e). Similar results are shown in Tagaris et al. (2007), who predicted a decrease of
623 23% as a result of decreasing emissions. In contrast, Avise et al. (2009) predicted an
624 average increase of 3 μg m^{-3} across the domain as a result of increasing NO_X and SO_2
625 from anthropogenic sources. Concentrations of SOA show an insignificant change as a
626 result of changes in anthropogenic emissions in the US. Similar to the scenario that
627 included changes in global anthropogenic emissions, these changes in SOA
628 concentrations are the result of small variations in the oxidant concentrations (Table 4).

629 In terms of the inorganic $PM_{2.5}$, reductions in SO_2 and NO_X emissions in the US
630 result in less than 5% decrease in SO_4^{2-} in most regions except for the Northwest and
631 Southwest, for which a slight increase of 1.5% is predicted (Table 3). Due to higher
632 emissions of NH_3, more sulfate aerosol is likely to be present in the form of ammonium
633 sulfate. When compared to Tagaris et al. (2007), our investigation shows a lower
634 reduction in SO_4^{2-} concentrations as a result of smaller reduction in SO_2 emissions from
635 anthropogenic sources.

636 **3.4.2 Contribution to PM2.5 concentrations from global climate change alone**

637 Despite the effect of precipitation on PM loading, as it washes out the precursors
638 and the existing PM from the atmosphere (Seinfeld and Pandis, 2006), the effect of
639 climate change alone (with no change to biogenic emissions) on total $PM_{2.5}$
640 concentrations over land is insignificant (Figure 11b). However, the change in $PM_{2.5}$
641 composition due to climate change is highly variable and depends on changes in
642 temperature, relative humidity and precipitation. Increases in reaction rate constants of
643 SO_2 and higher oxidant concentrations from increased temperature and solar insolation

lead to an increase in aerosol sulfate formed and thus are correlated with changes in SO_4^{2-} concentrations (Dawson et al., 2007). Relative humidity and temperature affect the thermodynamic equilibrium of SO_4^{2-}-NH_4^+-NO_3^-, especially the partitioning of HNO_3 between the gas and particulate phases.

For all regions, except for the Northwest, sulfate concentrations are predicted to increase by 3-8%. This change in concentrations is consistent with decreased precipitation, which reduces wet deposition. Increases in temperature and solar insolation, which increase radical production rates, increases the oxidation of SO_2 to produce aerosol sulfate. The same increase in temperature leads to nitrate being more volatile and thus decreases aerosol nitrate concentrations in all regions where sulfate concentrations are predicted to increase. An exception is in the Southwest, where sulfate, nitrate, and ammonium are all predicted to increase, likely due to the effect of a substantial decrease in precipitation (>60%). For the same regions where SO_4^{2-} is projected to increase, higher concentrations of radicals also lead to higher oxidation of VOC, thus increasing SOA concentrations in the same regions.

Reduced relative humidity in addition to an increase in temperature leads to decreased partitioning of ammonia to ammonium aerosol. This reduction is observed in most of the domain, except for the Northwest region and the northern boundary of the Central region where relative humidity is predicted to increase.

While increasing precipitation is generally associated with decreasing $PM_{2.5}$, results here for the urban and coastal areas in the Northwest and Southwest showed a

small increase in $PM_{2.5}$ despite an increase in precipitation (Figure 11b). This suggests the effects of slightly colder temperature and higher relative humidity in this region, leading to an enhanced formation of $(NH_4)NO_3$ (Table 3). Higher concentrations of (NH4)NO3, in addition to higher concentrations of SOA (Table 4), appear to dominate over the effect of precipitation.

3.4.3 Contribution to $PM_{2.5}$ concentrations from changes in biogenic emissions and future land use

Simulations that consider projected climate change as well as the associated change in biogenic emissions (Simulation 2) show an increase in $PM_{2.5}$ between 0.5 and 2 μg m^{-3}. These changes are mainly reflected in areas with high biogenic sources (Figures 11c and 11d). When the effects of future land use are considered (Simulation 3), an increase in the geographical extent of $PM_{2.5}$ is observed in comparison to the climate and biogenic emissions case, and higher increases (up to 2 μg m^{-3}) of $PM_{2.5}$ are predicted in parts of the Midwest, South and Northeast regions. This is primarily due to the increase in emissions of sesquiterpenes and monoterpenes (Figure 9b), leading to more SOA being formed.

In terms of the inorganic components of $PM_{2.5}$, the effect of climate change is still the predominant factor for the change in SO_4^{2-} concentrations across the domain (Table 3). The increase in SO_4^{2-} is less in comparison to the climate-only case due to the competition between BVOC and SO_2 for the availability of OH, which is an oxidant for both. Additionally, more pronounced decreases in NO_3^- are observed in the South, Northeast and Southwest than in the climate-only simulation. This is mainly due to the formation of organic nitrates in the presence of increased VOC, leading to a reduction in

the formation of HNO_3 (not shown) that can condense to form aerosol NO_3^-. In contrast, the Southwest and Northwest regions experience an increase in NH_4^+ and NO_3^- concentrations in the same amount as the climate-only case, which suggests that changes in both species are mostly driven by the changes in the meteorological fields.

SOA concentrations are predicted to increase as a result of higher emissions of BVOC across the domain. Furthermore, when climate change and biogenic emissions are combined with future land use, concentrations of SOA are predicted to increase up to 121% in the Central region and up to 188% in the Southeast due to increased monoterpene, and sesquiterpene emissions (not shown).

3.4.4 Changes in Precursors and $PM_{2.5}$ Concentrations from the Combined Global Changes

Table 5 shows the summary of changes to $PM_{2.5}$ as a result of the individual and combined global changes presented above. The differences in $PM_{2.5}$ between the future decade and current decade base case are greater in the eastern half of the US compared to the western half. In the eastern half of the US, the largest increases in $PM_{2.5}$ occur in the Southeast (with the exception of Florida, which shows a decrease), while the Northeast region exhibits the largest decrease. Our results show that the 0.5 to 2 μg m^{-3} increase in $PM_{2.5}$ in the Southeast region is dominated by higher concentrations of SOA due to increased biogenic emissions as a result of climate change (Figure 11c) and changes in land use (Figure 11d; Table 4). Table 3 indicates that with the exception of the Northwest region, which experienced a reduction in SO_4^{2-} due to decreased temperature, regions with a predicted decrease in inorganic $PM_{2.5}$ are dominated by reductions in NH_4^+ and NO_3^-. These reductions in inorganic aerosol

concentrations result from the combined effects of changes in weather patterns and reductions in regional anthropogenic precursors.

4. Conclusions

We have investigated the individual and combined contributions of factors that impact US air quality by dynamically downscaling future climate projections using the WRF model and using the regional chemical transport model CMAQ version 4.7.1. Decreases in future US anthropogenic ozone and $PM_{2.5}$ precursor emissions are the only consistently positive influences (reduced concentrations) on air quality in the US. However, in the case of ozone, that effect is offset by 1) changes in long range transport and increasing Asian and Mexican emissions, which have a negative impact on air quality across the domain; 2) climate changes (namely, increased temperatures and solar radiation) which increase ozone concentrations in the Central, South, Midwest, and East regions of the domain; and 3) increases in US BVOC emissions which also increase ozone concentrations in regions with high biogenic emissions.

In the case of the overall concentrations of $PM_{2.5}$, our results indicate that only the effects of increasing biogenic emissions have a negative impact on air quality by increasing $PM_{2.5}$ concentrations. In terms of the $PM_{2.5}$ composition, we show a regionally dependent mixture of inorganic aerosols and SOA. For the case of the Southeast, our findings indicate that increases in BVOC will result in higher concentrations of $PM_{2.5}$. This effect extends to the Midwest and Northeast regions due to changes in land use. Furthermore, meteorological changes or regulatory curtailment,

732 as incorporated in these simulations do not offset the increasing concentrations of SOA.
733 On the contrary, synergistic effects of changes in meteorological parameters and
734 emission reductions will shift the composition of the inorganic fraction of $PM_{2.5}$ in the
735 western US. However, an increase of NO_3^- and SOA in the urban areas of the coastal
736 regions of the Northwest and Southwest leads to an increase in $PM_{2.5}$ in those regions,
737 apparently off-setting decreases due to increased precipitation and temperature, and
738 reduced anthropogenic emissions.

739 In conclusion, this study suggests that the efforts to improve air quality through
740 low emission technologies and public policy will have a major effect in heavily populated
741 areas. However, higher global anthropogenic emissions, a warmer future world and the
742 effects of these changes on emissions from biogenic sources will undermine those
743 efforts. Consequently, additional measures will be necessary to improve air quality in
744 the US.

745 Much of the modeling components used for this research carry different levels of
746 complexity and have reached diverse stages of development, thus, subsequent
747 research intended so asses the effect of climate change and future regional emissions
748 upon air quality would benefit from newer versions of the emission inventories (e.g.
749 2011); updated assumptions on the US emission projections (e.g. New versions of
750 MARKAL with the use of the ESP 2.0 methodology); newer versions of MEGAN that
751 takes into account the isoprene emission suppression due to CO_2 concentrations and;
752 the inclusion of emissions from wildfires and the consequent effect upon air quality.

Acknowledgments

This work was supported by the U.S. Environmental Protection Agency Science To Achieve Results Grants RD 83336901-0 and 838309621-0. This paper has been cleared by the EPA's administrative review process and approved for publication. The views expressed in this paper are those of the authors and do not necessarily reflect the views or policies of the US Environmental Protection Agency.

References

Alcamo, J: IMAGE 2.0 : integrated modeling of global climate change, Kluwer Academic, Dordrecht., 1994.

Ambrose, J.L., Reidmiller, D.R., and Jaffe, D.A.: Causes of high O3 in the lower free troposphere over the Pacific Northwest as observed at the Mt. Bachelor Observatory. Atmos. Environ., 45, 5302–5315, 2011.

Appel, K. W., Chemel, C., Roselle, S. J., Francis, X. V., Hu, R. M., Sokhi, R. S., Rao, S. T. and Galmarini, S.: Examination of the Community Multiscale Air Quality (CMAQ) model performance over the North American and European domains, Atmos. Environ., 53, 142-155, 2012.

Avise, J., Abraham, R. G., Chung, S. H., Chen, J., Lamb, B., Salathé, E. P., Zhang, Y., Nolte, C. G., Loughlin, D. H. and Guenther, A.: Evaluating the effects of climate change on summertime ozone using a relative response factor approach for policymakers, J. Air Waste. Manage., 62(9), 1061–1074, 2012.

Avise, J., Chen, J., Lamb, B., Wiedinmyer, C., Guenther, A., Salathé, E. and Mass, C.: Attribution of projected changes in summertime US ozone and PM2. 5 concentrations to global changes, Atmos. Chem. Phys., 9, 1111–1124, 2009.

Aw, J. and Kleeman, M. J.: Evaluating the first-order effect of intraannual temperature variability on urban air pollution, J. Geophys. Res., 108(D12), 4365, 2003.

Bond, T. C., Streets, D. G., Yarber, K. F., Nelson, S. M., Woo, J. H. and Klimont, Z.: A technology-based global inventory of black and organic carbon emissions from combustion, J. Geophys. Res., 109(D14), D14203, 2004.

Boylan, J. W. and Russell, A. G.: PM and light extinction model performance metrics, goals, and criteria for three-dimensional air quality models, Atmos. Environ., 40(26), 4946–4959, 2006.

Byun, D. and Schere, K. L.: Review of the governing equations, computational algorithms, and other components of the Models-3 Community Multiscale Air Quality (CMAQ) modeling system, Appl. Mech. Rev., 59(1/6), 51, 2006.

Carlton, A. G., Bhave, P. V., Napelenok, S. L., Edney, E. O., Sarwar, G., Pinder, R. W., Pouliot, G. A. and Houyoux, M.: Model representation of secondary organic aerosol in CMAQv4. 7, Environ. Sci. Technol., 44(22), 8553–8560, 2010.

Carter, W. P. L. :A detailed mechanism for the gas-phase atmospheric reactions of organic compounds, Atmos. Environ., Part A, General Topics 24, 481e518, 1990.

Carter, W.P.L.: Documentation of the SAPRC-99 Chemical Mechanism for VOC Reactivity Assessment. Report to the California Air Resources Board. Available at: http://cert.ucr.edu/wcarter/absts.htm#saprc99; http://www.cert.ucr.edu/ wcarter/reactdat.htm, 2000.

Chen, J., Avise, J., Guenther, A., Wiedinmyer, C., Salathe, E., Jackson, R. B. and Lamb, B.: Future land use and land cover influences on regional biogenic emissions and air quality in the United States, Atmos. Environ., 43(36), 5771 – 5780, doi:10.1016/j.atmosenv.2009.08.015, 2009a.

Chen, J., Avise, J., Lamb, B., Salathé, E., Mass, C., Guenther, A., Wiedinmyer, C., Lamarque, J. F., O'Neill, S. and McKenzie, D.: The effects of global changes upon regional ozone pollution in the United States, Atmos. Chem. Phys, 9, 1125–1141, 2009b.

Christensen, J.H., B. Hewitson, A. Busuioc, A. Chen, X. Gao, I. Held, R. Jones, R.K. Kolli, W.-T. Kwon, R. Laprise, V. Magaña Rueda, L. Mearns, C.G. Menéndez, J. Räisänen, A. Rinke, A. Sarr and P. Whetton, 2007: Regional Climate Projections. In: Climate Change.: The Physical Science Basis. Contribution of Working Group I to the Fourth Assessment Report of the Intergovernmental Panel on Climate Change [Solomon, S., D. Qin, M. Manning, Z. Chen, M. Marquis, K.B. Averyt, M. Tignor and H.L. Miller (eds.)]. Cambridge University Press, Cambridge, United Kingdom and New York, NY, USA, 2007.

Dadvand, P., Parker, J., Bell, M.L., Bonzini, M., Brauer, M., Darrow, L., Gehring, U., Glinianaia, S.V., Gouveia, N., Ha, E.-H., et al.: Maternal Exposure to Particulate Air Pollution and Term Birth Weight: A Multi-Country Evaluation of Effect and Heterogeneity. Environ. Health Persp., 2012.

Dawson, J. P., Adams, P. J. and Pandis, S. N.: Sensitivity of $PM_{2.5}$ to climate in the Eastern US: a modeling case study, Atmos. Chem. Phys., 7, 4295–4309, 2007.

Dawson, J. P., Bloomer, B. J., Winner, D. A. and Weaver, C. P.: Understanding the meteorological drivers of U.S. particulate matter concentrations in a changing climate, Bull. Amer. Meteor. Soc., doi:10.1175/BAMS-D-12-00181.1, 2013.

Dulière, V., Zhang, Y. and Salathé Jr., E. P.: Changes in twentieth-century extreme temperature and precipitation over the western United States based on observations and regional climate model simulations. J. Climate, 26, 8556-8575, doi:10.1175/JCLI-D-12-00818.1, 2013.

Dulière, V., Zhang, Y. and Salathé Jr., E. P.: Extreme Precipitation and Temperature over the U.S. Pacific Northwest: A Comparison between Observations, Reanalysis Data, and Regional Models, J. Climate, 24(7), 1950–1964, doi:10.1175/2010JCLI3224.1, 2011.

Fiore, A. M., West, J. J., Horowitz, L. W., Naik, V. and Schwarzkopf, M. D.: Characterizing the tropospheric ozone response to methane emission controls and the benefits to climate and air quality, J. Geophys. Res., 113, D08307, doi:10.1029/2007JD009162, 2008.

Foley, K. M., Roselle, S. J., Appel, K. W., Bhave, P. V., Pleim, J. E., Otte, T. L., Mathur, R., Sarwar, G., Young, J. O., Gilliam, R. C., Nolte, C. G., et al.: Incremental testing of the Community Multiscale Air Quality (CMAQ) modeling system version 4.7, Geoscientific Model Development, 3(1), 205–226, doi:10.5194/gmd-3-205-2010, 2010.

Fountoukis, C. and Nenes, A.: ISORROPIA II: a computationally efficient thermodynamic equilibrium model for K+–Ca2+–Mg2+–NH, Atmos. Chem. Phys, 7, 4639–4659, 2007.

Forkel, R. and Knoche, R.: Regional climate change and its impact on photooxidant concentrations in southern Germany: Simulations with a coupled regional climate-chemistry model, J. Geophys. Res., 111(D12), doi:10.1029/2005JD006748, 2006.

Giorgi, F. and Meleux, F.: Modelling the regional effects of climate change on air quality, C. R. Geosci., 339(11–12), 721 – 733, doi:http://dx.doi.org/10.1016/j.crte.2007.08.006, 2007.

Granier, C., J.F. Lamarque, A. Mieville, J.F. Muller, J. Olivier, J. Orlando, J. Peters, G. Petron, G. Tyndall, S. Wallens.: POET a database of surface emissions of ozone precursors, available on internet at http://www.aero.jussieu.fr/projet/ACCENT/POET.php, (accessed on 2005).

Grell, G. A., Dudhia, J., and Stauffer, D. R.: A Description of the Fifth-Generation Penn tate/NCAR Mesoscale Model (MM5), National Center for Atmospheric Research, Boulder, CO, USA, NCAR/TN-398+STR., 122 pp, 1994.

Guenther, A., T. Karl, P. Harley, C. Wiedinmyer , P. I. Palmer, C. Geron.: Estimates of global terrestrial isoprene emissions using MEGAN (Model of Emissions of Gases and Aerosols from Nature), Atmos. Chem. Phys., 6, 3181-3210, 2006.

Guenther, A. B., X. Jiang, C. L. Heald, T. Sakulyanontvittaya, T. Duhl, L. K. Emmons, and X. Wang: The Model of Emissions of Gases and Aerosols from Nature version 2.1 (MEGAN2.1): an extended and updated framework for modeling biogenic emissions, Geoscience Model Development, 5(6), 1471-1492. 2012.

Guenther, A.: Biological and Chemical Diversity of Biogenic Volatile Organic Emissions into the Atmosphere, ISRN Atmospheric Sciences, doi: 10.1155/2013/786290). 2013.

Heald, C. L., M. J. Wilkinson, R. K. Monson, C. A. Alo, G. Wang, and A. Guenther.: Response of isoprene emission to ambient CO2 changes and implications for global budgets, Global Change Biol., 15, 1127-1140., 2009.

Hogrefe, C., Lynn, B., Civerolo, K., Ku, J. Y., Rosenthal, J., Rosenzweig, C., Goldberg, R., Gaffin, S., Knowlton, K. and Kinney, P. L.: Simulating changes in regional air pollution over the eastern United States due to changes in global and regional climate and emissions, J. Geophys. Res., 109(D22), D22301, 2004.

Horowitz, L. W.: Past, present, and future concentrations of tropospheric ozone and aerosols: Methodology, ozone evaluation, and sensitivity to aerosol wet removal, J. Geophys. Res., 111(D22), D22211, 2006.

Huang, H.-C., Liang, X.-Z., Kunkel, K. E., Caughey, M. and Williams, A.: Seasonal Simulation of Tropospheric Ozone over the Midwestern and Northeastern United States: An Application of a Coupled Regional Climate and Air Quality Modeling System, J. Appl. Meteor. Climatol., 46(7), 945–960, doi:10.1175/JAM2521.1, 2007.

Huang, H.-C., Lin, J., Tao, Z., Choi, H., Patten, K., Kunkel, K., Xu, M., Zhu, J., Liang, X.-Z., Williams, A., Caughey, M., Wuebbles, D. J. and Wang, J.: Impacts of long-range transport of global pollutants and precursor gases on U.S. air quality under future climatic conditions, J. Geophys. Res,113(D19), n/a–n/a, doi:10.1029/2007JD009469, 2008.

Intergovernmental Panel on Climate Change and Intergovernmental Panel on Climate Change: Climate change 2007: the physical science basis: contribution of Working Group I to the Fourth Assessment Report of the Intergovernmental Panel on Climate Change, Cambridge University Press, Cambridge ; New York., 2007.

Jacob, D. J. and Winner, D. A.: Effect of climate change on air quality, Atmos. Environ., 43(1), 51 – 63, doi:10.1016/j.atmosenv.2008.09.051, 2009.

Karl, T. R., J. C.N. Williams, F. T. Quinlan, and T.A. Boden..: United States Historical Climatology Network (HCN) Serial Temperature and Precipitation Data. Vol. 3404, Environmental Science Division Publication, Carbon Dioxide Information and Analysis Center, Oak Ridge National Laboratory, 389 pp, 1990

Kelly, J., Makar, P. A., and Plummer, D. A.: Projections of mid-century summer air-quality for North America: effects of changes in climate and precursor emissions, Atmos. Chem. Phys., 12, 5367–5390, doi:10.5194/acp-12-5367-2012, 2012.

Kim, Y.P., Seinfeld, J.H., and Saxena, P.: Atmospheric gas-aerosol equilibrium I. Thermodynamic model. Aerosol Sci. Tech., 19, 157–181, 1993.

Kunkel, K. E., Huang, H. C., Liang, X. Z., Lin, J. T., Wuebbles, D., Tao, Z., Williams, A., Caughey, M., Zhu, J. and Hayhoe, K.: Sensitivity of future ozone concentrations in the northeast USA to regional climate change, Mitigation Adapt. Strategies Global Change, 13(5), 597–606, 2007.

Langner, J., Bergstrom, R. and Foltescu, V.: Impact of climate change on surface ozone and deposition of sulphur and nitrogen in Europe, Atmos. Environ., 39(6), 1129–1141, doi:10.1016/j.atmosenv.2004.09.082, 2005.

Lelieveld, J., and Dentener, F.: What controls tropospheric ozone? J. Geophys. Res., 105, 3531-3551, 2009

Leung, L. R. and Gustafson, W. I.: Potential regional climate change and implications to US air quality, Geophys. Res. Lett., 32, L16711, 2005.

Leung L.R., Kuo Y.H., Tribbia J.: Research needs and directions of regional climate modeling using WRF and CCSM. B Am Meteorol Soc., 87,1747–1751, 2006

Liao, H., Chen, W. T. and Seinfeld, J. H.: Role of climate change in global predictions of future tropospheric ozone and aerosols, J. Geophys. Res., 111(D12), D12304, 2006.

Liang, X.-Z., Pan, J., Zhu, J., Kunkel, K. E., Wang, J. X. L. and Dai, A.: Regional climate model downscaling of the U.S. summer climate and future change, J. Geophys. Res., 111(D10), doi:10.1029/2005JD006685, 2006.

Lin, J.-T., Patten, K.O., Hayhoe, K., Liang, X-Z., Wuebbles, D.J.: Effects of future climate and biogenic emissions changes on surface ozone over the United States and China, J. Appl. Meteor. Climatol, 47, 1888-1909, 2008.

Loughlin, D.H., Benjey, W.G. and Nolte, C.G.: ESP 1.0: Methodology for exploring emission impacts of future scenarios in the United States, Geoscientific Model Development, 4, 287-297, 2011.

Loulou R, G. Goldstein and K. Noble. 2004. Documentation for the MARKAL family of models. Energy Technology Systems Analysis Programme: Paris, France. http://www.etsap.org/tools.htm. (Accessed September 15, 2011)

Luo, C., Wang, Y., Mueller, S. and Knipping, E.: Diagnosis of an underestimation of summertime sulfate using the Community Multiscale Air Quality model, Atmos. Environ., 45(29), 5119–5130, 2011.

Meleux, F., Solmon, F., Giorgi, F.: Increase in summer European ozone amounts due to climate, Atmos. Environ., 7577–7587, 2007.

Nakicenovic, N., et al.: IPCC Special Report on Emissions Scenarios. Cambridge, UK: Cambridge University Press, 2000.

Neilson, R. P.: A Model for Predicting Continental-Scale Vegetation Distribution and Water Balance. Ecol. Appl., 5(2), 362-385, 1995

Nolte, C. G., Gilliland, A. B., Hogrefe, C. and Mickley, L. J.: Linking global to regional models to assess future climate impacts on surface ozone levels in the United States, J. Geophys. Res, 113, D14307, 2008.

Otte, T. L. and Pleim, J. E.: The Meteorology-Chemistry Interface Processor (MCIP) for the CMAQ modeling system: updates through MCIPv3.4.1, Geoscientific Model Development, 3(1), 243–256, doi:10.5194/gmd-3-243-2010, 2010.

Racherla, P. N. and Adams, P. J.: The response of surface ozone to climate change over the Eastern United States, Atmos. Chem. Phys., 8, 871–885, 2008.

Raes, F., Liao, H., Chen, W. T. and Seinfeld, J. H.: Atmospheric chemistry-climate feedbacks, J. Geophys. Res., 115(D12), D12121, 2010.

Ramankutty, N., Foley, J.A., Norman, J., and K. McSweeney.: The global distribution of cultivable lands: Current patterns and sensitivity to possible climate change, Global Ecol. Biogeogr, 11, 377-392, 2002.

Ramankutty, N., and J.A. Foley.: Characterizing patterns of global land use: An analysis of global croplands data, Global Biogeochem. Cy., 12(4), 667-685, 1998.

Ravishankara, A. R., Dawson, J. P. and Winner, D. A.: New Directions: Adapting air quality management to climate change: A must for planning, Atmos. Environ., 50(0), 387 – 389, doi:http://dx.doi.org/10.1016/j.atmosenv.2011.12.048, 2012.

Roeckner E., Bengtsson L., Feichter J., Lelieveld J., Rodhe H.: Transient climate change simulations with a coupled atmosphere-ocean GCM including the tropospheric sulfur cycle, J. Climate, (12)3004-3032, 1999.

Roeckner E, Bauml G, Bonaventura L, Brokopf R, Esch M, Giorgetta M, Hagemann S, Kirchner I, Kornbleuh L, Manzini E, Rhodin A, Schelse U, Schulzweida U, Tomkins A.: The atmospheric general circulation model ECHAM5, Part I: model description, Max-Planck Institute of Meteorology Report No. 349, 2003.

Rosenstiel, T. N., M. J. Potosnak, K. L. Griffin, R. Fall, and R. K. Monson.: Increased CO2 uncouples growth from isoprene emission in an agriforest ecosystem. Nature, 421 (6920), 256– 259, 2003.

Sakulyanontvittaya, T., T. Duhl, C. Wiedinmyer, D. Helmig, S. Matsunaga, M. Potosnak, J. Milford, and A. Guenther.: Monoterpene and sesquiterpene emission estimates for the United States, Environ. Sci. Tech., 42(5), 1623-1629. 2008

Salathé, E., Leung, L., Qian, Y. and Zhang, Y.: Regional climate model projections for the State of Washington, Climatic Change, 102(1), 51–75, 2010.

Seinfeld, J. H., & Pandis, S. N.: Atmospheric Chemistry and Physics: From air pollution to climate change (2nd Edition ed.), New Jersey: John Wiley and Sons, Inc, 2006.

Shay, C.L., Yeh, S., Decarolis, J., Loughlin, D.H., Gage, C.L. and Wright, E.: EPA U.S. National MARKAL Database: Database Documentation. U.S. Environmental Protection Agency, Washington, DC, EPA/600/R-06/057, 2006.

Steiner, A. L., S. Tonse, R. C. Cohen, A. H. Goldstein, and R. A. Harley.: Influence of future climate and emissions on regional air quality in California, J. Geophys. Res., 111, D18303, 2006

Tagaris, E., Manomaiphiboon, K., Liao, K.-J., Leung, L. R., Woo, J.-H., He, S., Amar, P. and Russell, A. G.: Impacts of global climate change and emissions on regional ozone and fine particulate matter concentrations over the United States, J. Geophys. Res.: Atmospheres, 112(D14), doi:10.1029/2006JD008262, 2007.

Tao, Z., Williams, A., Huang, H. C., Caughey, M. and Liang, X. Z.: Sensitivity of US surface ozone to future emissions and climate changes, Geophys. Res. lett., 34(8), L08811, 2007.

Unger, N. Shindal, D.T., Koch, D.M., Amann, M., Cofala, J., Streets, D.G.: Influences of man- made emissions and climate changes in tropospheric ozone, methane and sulfate at 2030 from a broad range of possible futures. J. Geophys. Res., 111, D12313, 2006.

United States Code of Federal Regulations (US CFR). 2017-2025 model year light-duty vehicle GHG and 904 CAFE standards: supplemental notice of intent. United States 905. Federal Register 76(153) 2011.

U.S. Department of Energy. Energy Information Administration (US EIA). Annual Energy Outlook 2008 with Projections to 2030, DOE/EIA-0383(2008), U.S. Department of Energy: Washington, D.C., 2008.

U.S. Environmental Protection Agency (US EPA). Clean Air Interstate Rule emissions inventory technical support document, US Environmental Protection Agency, Office of Air Quality Planning and Standards, Research Triangle Park, NC, available at: http://www.epa.gov/cair/pdfs/finaltech01.pdf(last access: March 2011), 2005

US. Environmental Protection Agency (EPA): National Ambient Air Quality Standards for Ozone, Proposed Rule, Federal Register, 75(11), 2938-3052, 2010.

US Environmental Protection Agency (EPA): Quality assurance guidance document-Final quality assurance project plan: PM2.5 speciation trends network field sampling (EPA-454/R-01-001). US environmental protection agency, Office of air quality planning and standards, Research triangle park, NC, 2000.

U.S. Environmental Protection Agency (US EPA). Office of Research and Development. EPA U.S. Nine Region MARKAL Database: Database Documentation. NTIS number forthcoming. Research Triangle Park, N.C., 2013.

Washington, W. M., Weatherly, J. W., Meehl, G. A., Semtner, A. J., Bettge, T.W., Craig, A. P., Strand, W. G., Arblaster, J., Wayland, V. B., James, R., and Zhang, Y.: Parallel Climate Model (PCM) control and transient simulations. Climate Dyn., 16(10–11), 755–774, 2000.

Weaver, C. P., Cooter, E., Gilliam, R., Gilliland, A., Grambsch, A., Grano, D., Hemming, B., Hunt, S. W., Nolte, C., Winner, D. A., Liang, X.-Z., et al.: A Preliminary Synthesis of Modeled Climate Change Impacts on U.S. Regional Ozone Concentrations, Bull. Amer. Meteor. Soc., 90(12), 1843–1863, doi:10.1175/2009BAMS2568.1, 2009.

Wuebbles, D.J., Lei, H., and Lin, J.: Intercontinental transport of aerosols and photochemical oxidants from Asia and its consequences. Environ. Pollut., 150, 65–84, 2007.

World Health Organization (WHO): Air quality guidelines for particulate matter, ozone, nitrogen dioxide and sulfur dioxide: Summary of risk assessment. 2005

World Meteorological Organization (WMO): Global Atmosphere Watch: WMO/iGAC Impacts of Megacities on Air Pollution and Climate, 2012

Wu, S., Mickley, L.J., Leibensperger, E.M., Jacob, D.J., Rind, D., Streets, D.G.: Effects of 2000-2050 global change on ozone air quality in the United States. J. Geophys. Res., 113, D06302., 2008a

Wu, S., Mickley, L.J., Jacob, D.J., Rind, D., Streets, D.G.: Effects of 2000-2050 changes in climate and emissions on global tropospheric ozone and the policy-relevant background ozone in the United States. J. Geophys. Res., 113, D18312., 2008b

Xie, Y., Paulot, F., Carter, W. P. L., Nolte, C. G., Luecken, D. J., Hutzell, W. T., Wennberg, P. O., Cohen, R. C. and Pinder, R. W.: Understanding the impact of recent advances in isoprene photooxidation on simulations of regional air quality, Atmos. Chem. Phys., 13(16), 8439–8455, doi:10.5194/acp-13-8439-2013, 2013.

Zhang, Y., Qian, Y., Dulière, V., Salathé Jr., E. P., and Leung, L. R.: ENSO anomalies over the Western United States: present and future patterns in regional climate simulations, Climatic Change, 110(1-2), 315–346, doi:10.1007/s10584-011-0088-7, 2012.

Zhang, Y., Olsen, S. C., and Dubey, M. K.: WRF/Chem simulated springtime impact of rising Asian emissions on air quality over the U.S.. Atmos. Environ., 44, 2799-2812, 2010.

Zhang, Y., Dulière, V., and Salathé Jr., E. P.: Evaluation of WRF and HadRM mesoscale climate simulations over the United States Pacific Northwest. J. Climate, 22, 5511-5526, 2009.

Zhang, L., Jacob, D.J., Downey, N.V., Wood, D.A., Blewitt, D., Carouge, C.C., Van Donkelaar, A., Jones, D., Murray, L.T., and Wang, Y.: Improved estimate of the policy-

relevant background ozone in the United States using the GEOS-Chem global model with 1/2 times 2/3 horizontal resolution over North America. Atmos. Environ., 45, 6769–6776, doi:10.1016/j.atmosenv.2011.07.054, 2011

Zuidema, G., Born, G. J., Alcamo, J. and Kreileman, G. J. J.: Simulating changes in global land cover as affected by economic and climatic factors, Water Air and Soil Pollution, 76(1-2), 163–198, doi:10.1007/BF00478339, 1994.

Table 1. List of simulations to assess the effect of global climate changes upon air quality in the United States

	Climate	Biogenic Emissions		Anthropogenic Emissions	
		Climate	Land Use	US	Global
0	Current	Current	Current	Current	Current
1	**Future**	Current	Current	Current	Current
2	**Future**	**Future**	Current	Current	Current
3	**Future**	**Future**	**Future**	Current	Current
4	Current	Current	Current	**Future**	Current
5	Current	Current	Current	Current	**Future**
6	**Future**	**Future**	**Future**	**Future**	**Future**

Table 2. Regional effects upon DM8O for each change and the combined effects. + indicates an increase in concentrations, - indicates a decrease in concentrations, ~ indicates neither increase nor decrease, +/- indicates nonhomogeneous increase or decrease.

	Boundary Conditions	US emissions	Climate	BVOC	Combined Effects
Northwest	+	-	-	+/-	+
Southwest	+	-	+/-	+/-	+/-
Central	+	-	+	+/-	+
South	+	-	+	+/-	+
Midwest	+	-	+	+/-	+
Northeast	+	-	+	+/-	+
Southeast	+	-	+	+	+/-

Table 3. Percent change in the aerosol NH_4^+, SO_4^{2-} and NO_3^- between each future scenario and the current decade base case.

Region	Boundary Conditions	US emissions	BVOC	BVOC Future Land Use	Climate	Combined
			NH_4^+			
Northwest	-18.8	2.3	4.9	5.3	7.7	-10
Southwest	-10.6	3.0	10.1	11.1	11.7	3.5
Central	-18.7	0.2	5.4	7.5	3.1	-9.4
South	-12.4	0.6	-20.5	-17.2	-23.1	-28.8
Midwest	-20.5	-0.9	-8.1	-3.4	-13.4	-26
Northeast	-14.2	-0.3	-11.4	-8.1	-13.3	-24.8
Southeast	-12.3	1.3	-10.1	-7.6	-10.5	-19.2
			SO_4^{2-}			
Northwest	-4.8	1.5	-16.3	-16.2	-10.4	-18.5
Southwest	-2.1	1.5	-0.1	-0.4	4.2	-0.4
Central	-1.3	-1.4	1.3	2.7	7.7	-0.7
South	-2.1	-1.1	2.8	4.4	3.3	0.9
Midwest	-0.8	-4.9	2.0	6.8	7.9	0.9
Northeast	-0.8	-2.8	2.4	4.5	7.9	0.4
Southeast	-2.2	-1.7	4.5	6	7.1	1.8
			NO_3^-			
Northwest	10.9	-10.5	13.2	10.5	13.3	5.2
Southwest	9	-16.9	8	8.8	8.0	-1.8
Central	-5.6	-3.5	-1.2	-1.2	-16.1	-12.6
South	16.2	-2.7	-24.5	-23.5	-20.3	-14.2
Midwest	1.7	0.8	-42.7	-39.6	-47.7	-45.0
Northeast	4.7	-20.2	-16.3	-18.5	-8.6	-29.8
Southeast	9.7	-8.7	-14.0	-18.0	-11.5	-17

Table 4 Percent change of secondary organic aerosol and primary organic carbon between each future scenario and the current decade base case.

Region	Boundary Conditions	US emissions	BVOC	BVOC Future Land Use	Climate	Combined
SOA						
Northwest	0.3	0.1	19.8	29.8	12.0	30.6
Southwest	-1.0	-1.3	39.3	44.4	5.6	42.5
Central	-0.8	-0.4	55.8	121.6	12.6	118.6
South	-0.4	-1.3	83.3	151.6	5.4	149.5
Midwest	0.0	-2.4	65.9	164.8	13.9	166.7
Northeast	0.1	-2.4	73.7	141.6	14.8	137.1
Southeast	-0.1	-2.3	102.4	188.0	11.5	182.8

Table 5. Regional effect upon $PM_{2.5}$ from each change and the combined effects. + indicates an increase in concentrations, - indicates a decrease in concentrations, ~ indicates neither increase nor decrease, +/- indicates non homogeneous increase or decrease.

	Boundary Conditions	US emissions	Climate	BVOC	Combined Effects
Northwest	~	-/+	+	-	+
Southwest	~	-/+	+	~	+/-
Central	~	~	~	+	+/-
South	~	-/+	~	+	+/-
Midwest	~	-	~	+	+/-
Northeast	~	-	~	+	+
Southeast	~	-	+/-	+	+

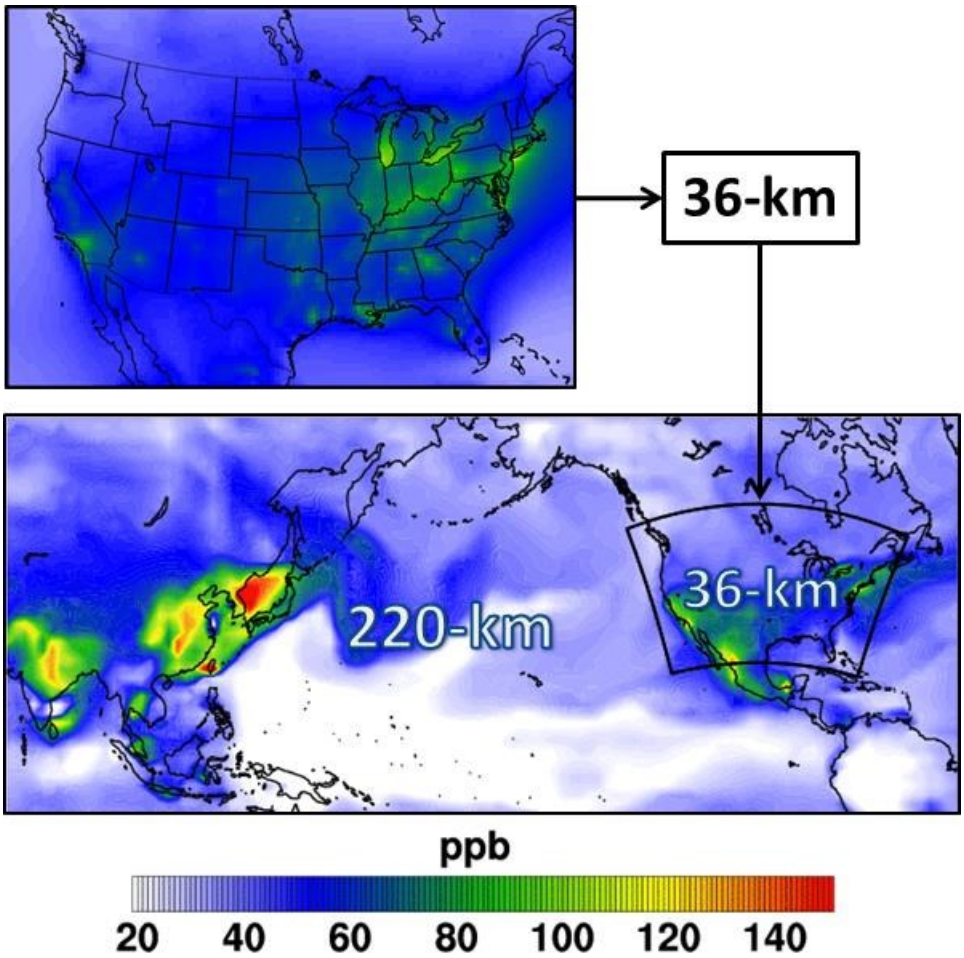

Figure 1. Projected future DM8O concentrations used to show the CMAQ modeling domains at 36 and 220 km resolutions. The 36 km modeling domain was nested inside the 220 km domain.

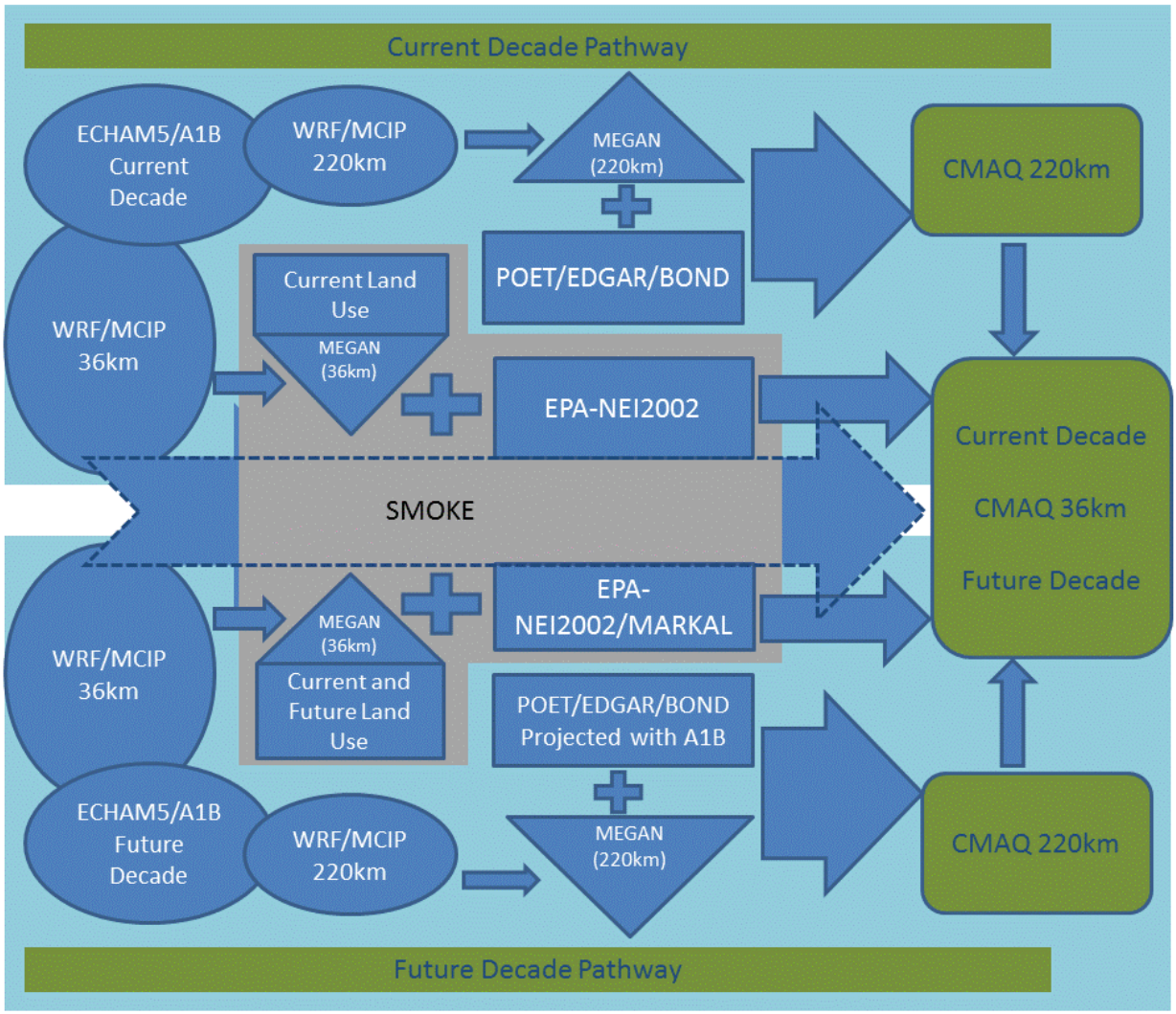

Figure 2. Schematic of the modeling framework.

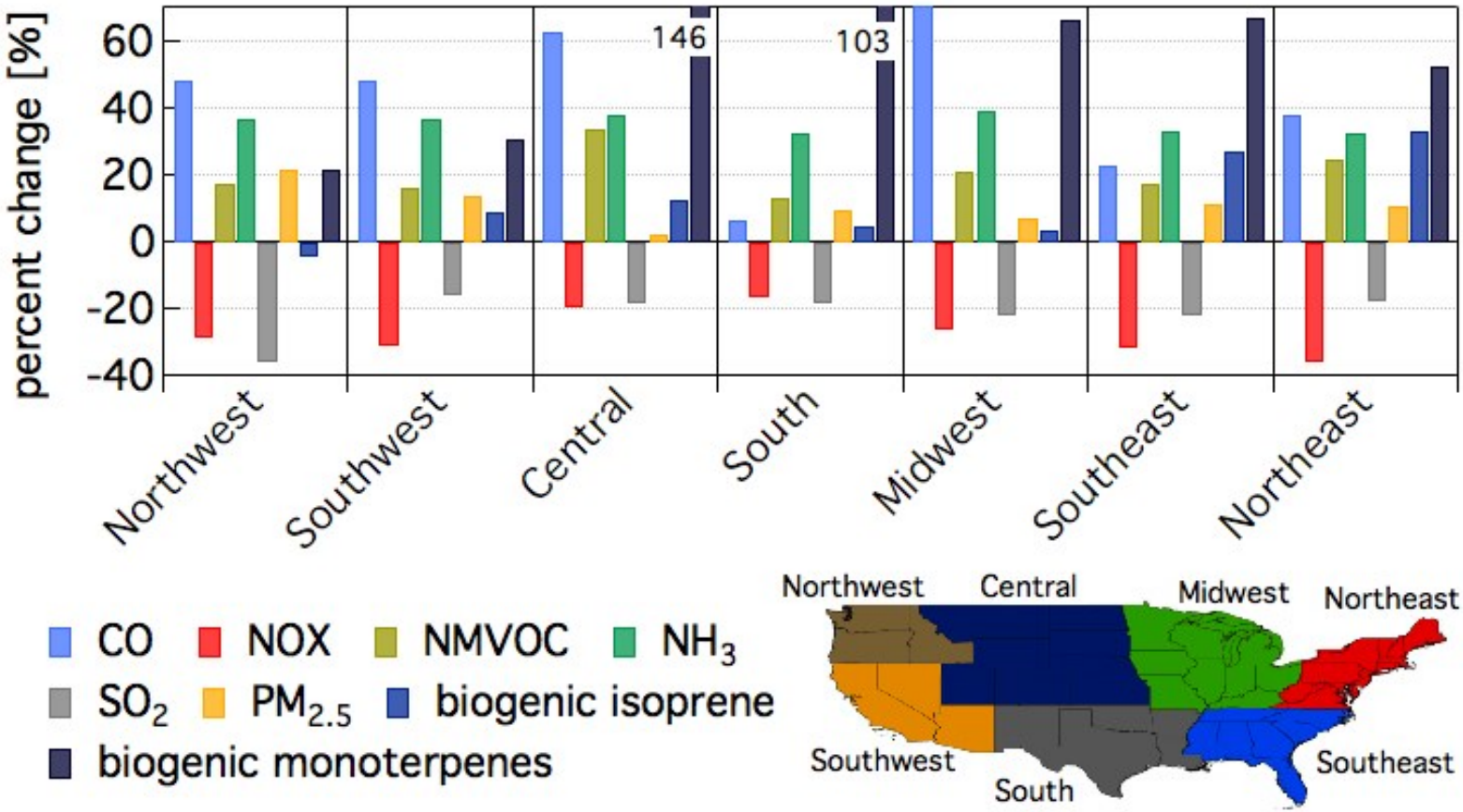

Figure 3. Summary of regional changes in US anthropogenic and biogenic emissions from future decade land use.

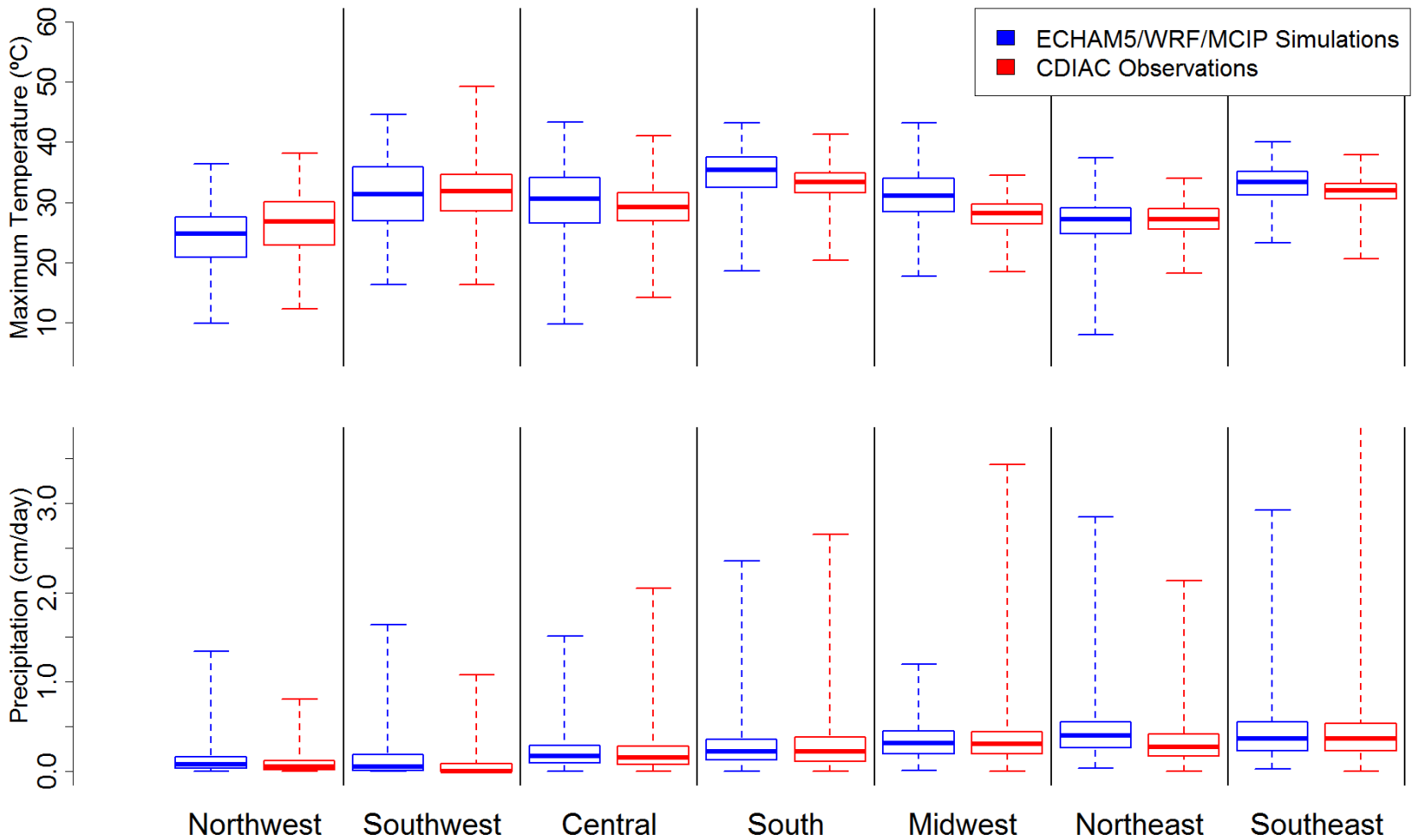

Figure 4. Comparison of modeled and observed seasonal-mean meteorological variables by region: maximum daily temperatures (top); and precipitation rates (bottom). Each box-and-whisker indicates median, 25% and 75% quartiles, maximums and minimums of the values across all sites within each region.

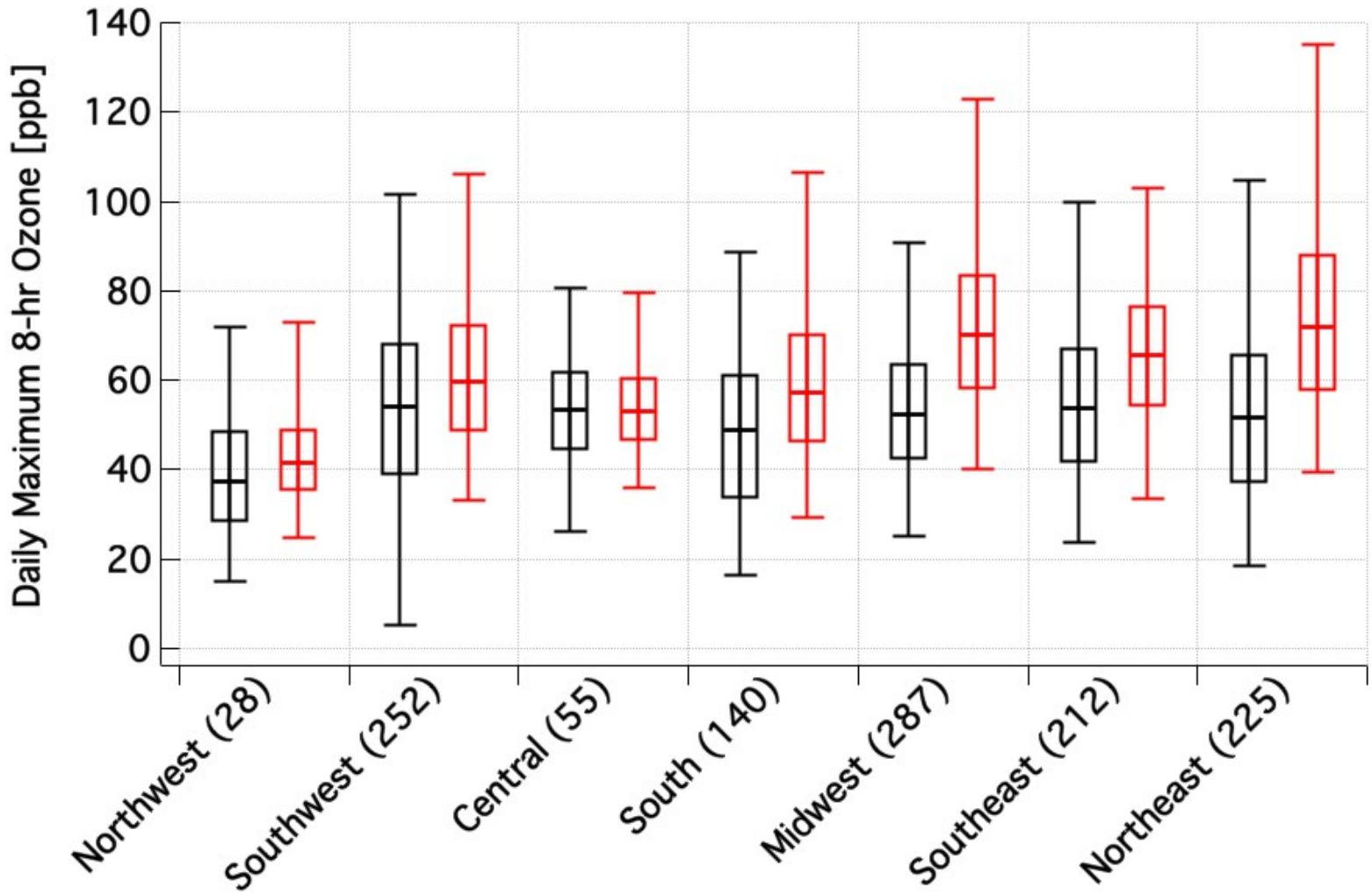

Figure 5. 2nd, 25th, 50th, 75th, 98th percentiles of observed (black) vs modeled (red) values of DM8O for each region. The number of monitoring stations per region is shown in parenthesis.

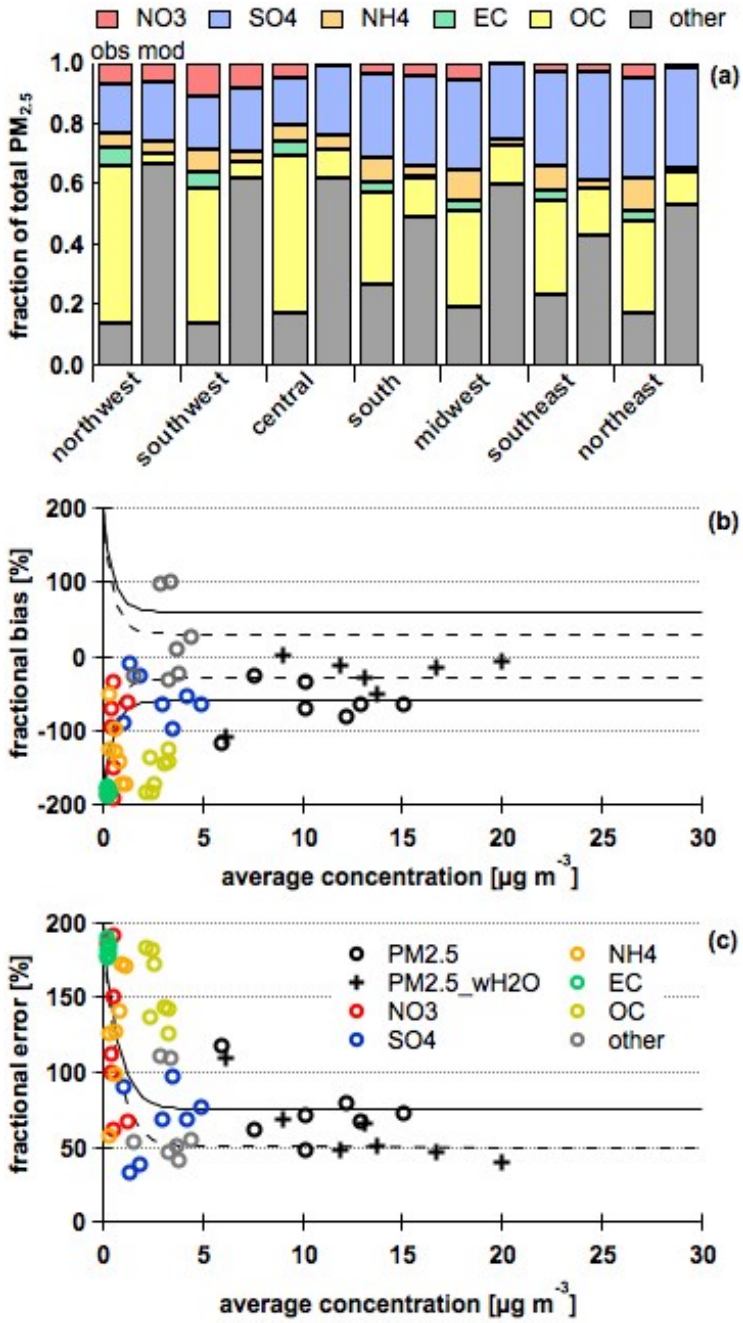

Figure 6. (Top Panel) Fraction from observed (left) and simulated current decade (right) $PM_{2.5}$ for each geographic region; (Middle Panel) Fractional bias goal (dashed lines) and criteria (solid lines) thresholds given in the EPA model performance guidance for the simulated $PM_{2.5}$ species; (Bottom Panel) Fractional error goal (dashed line) and criteria (solid line) given in the EPA model performance guidance for the simulated $PM_{2.5}$ species. Each point represents the "decade" average of the species 24hr average in each geographic region from figure 3.

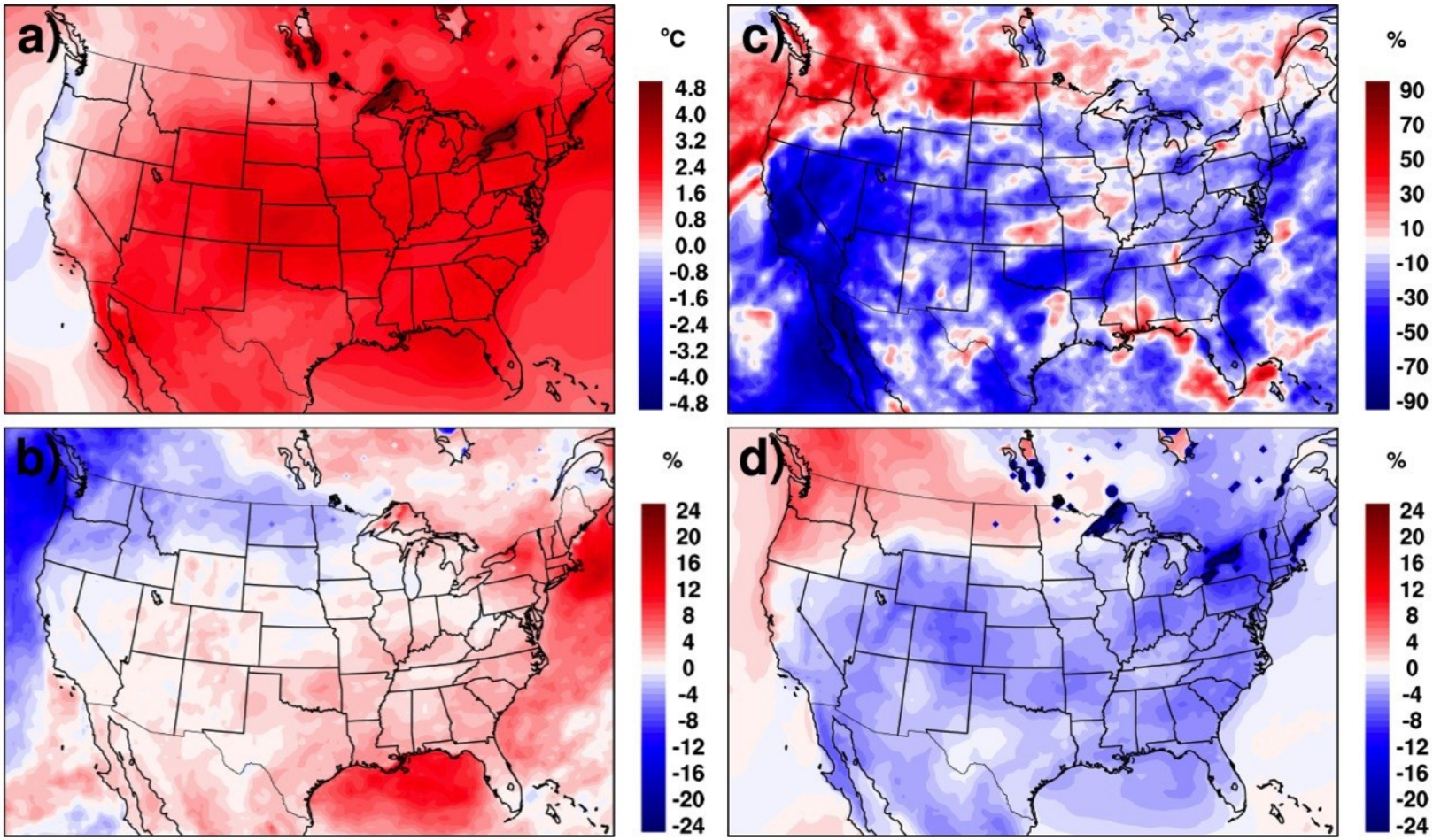

Figure 7 Projected changes in summertime meteorological fields (future decade - current decade): a) changes in 2-m temperature (^{o}C); b) percent change in solar radiation reaching the ground; c) percent change in precipitation; d) change in relative humidity.

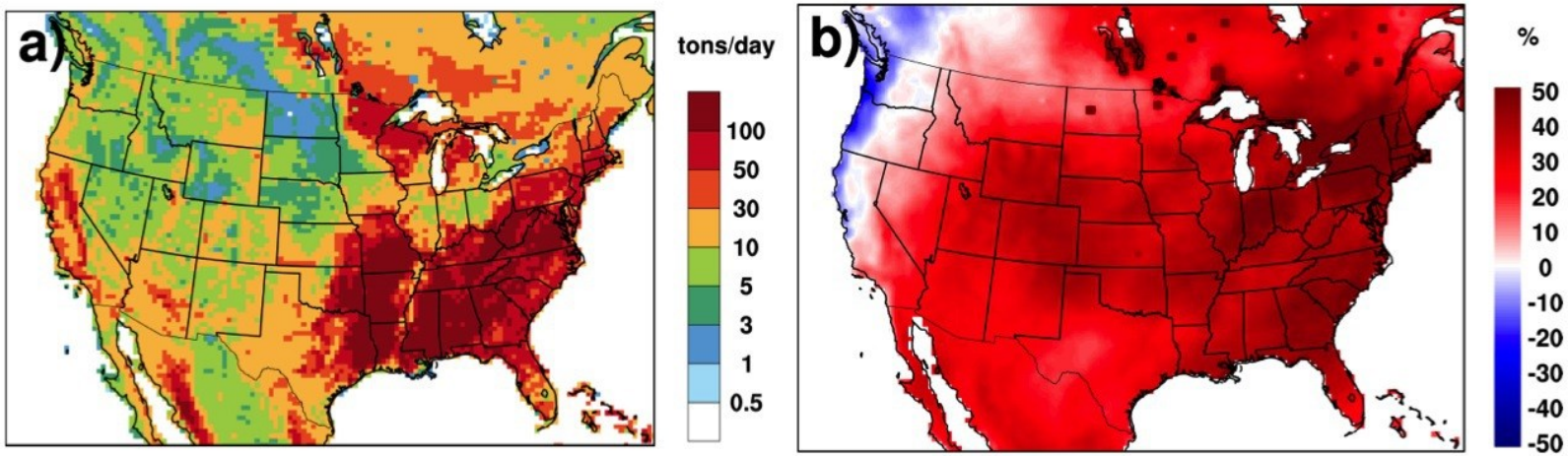

Figure 8. a) Current decade summertime isoprene emissions, and b) percent change induced by climate on future summertime isoprene emissions with current decade land use.

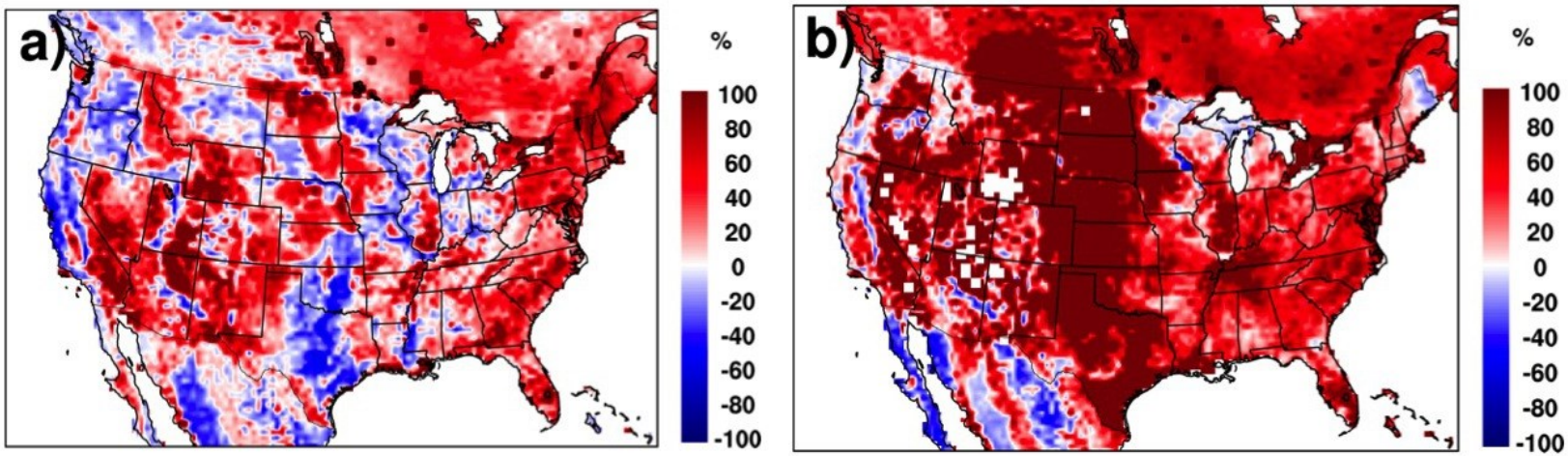

Figure 9. Percent change between future and current decade summertime emissions for future climate and land use for a) isoprene and b) monoterpene.

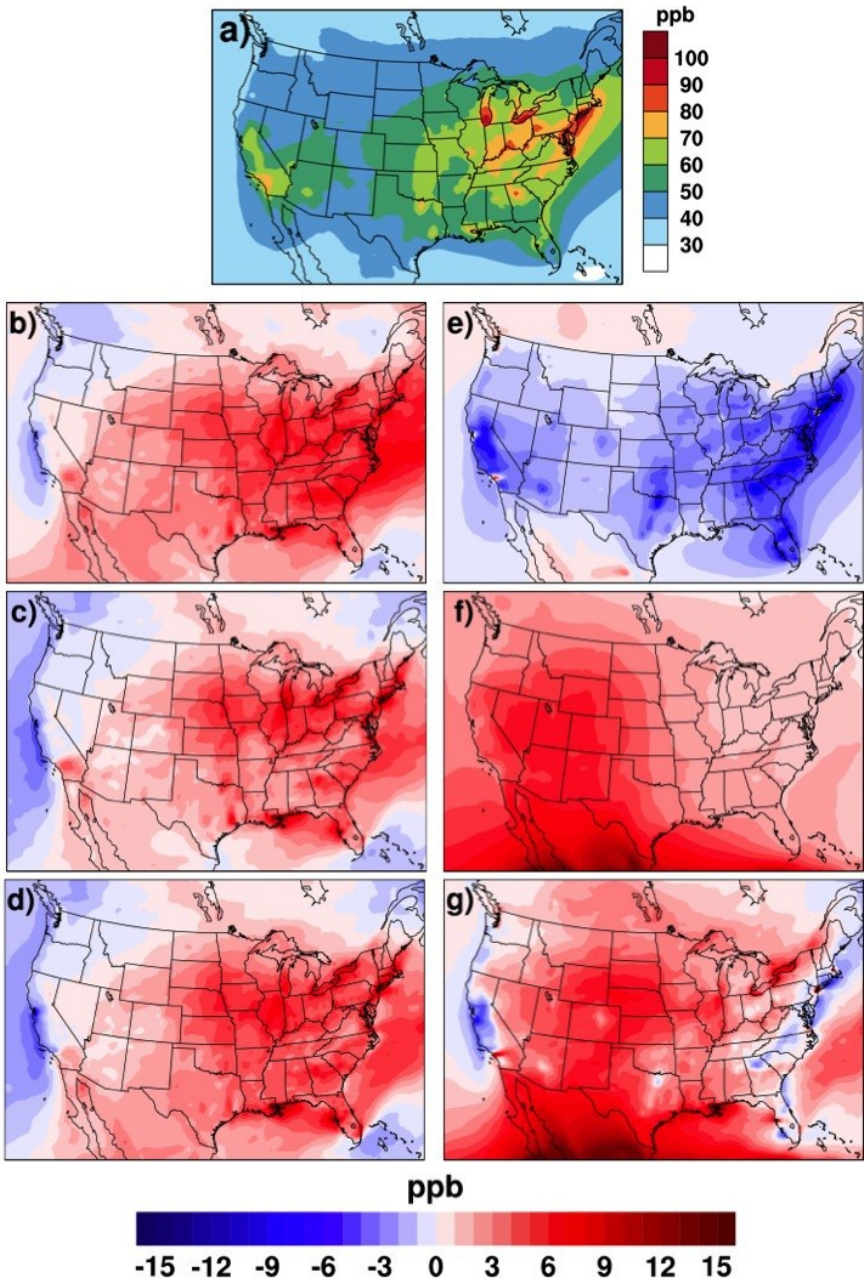

Figure 10. a) Current decade base case daily maximum 8-hour ozone average concentrations for five summers in the 2000s; spatial distribution and regional effect on maximum 8-hour ozone due to: b) changes in meteorology (Simulation 1); c) changes in meteorology and biogenic emissions (Simulation 2); d) changes in meteorology, biogenic emissions, and land use (Simulation 3); e) changes in US anthropogenic emissions (Simulation 4); f) changes in global anthropogenic emissions (Simulation 5); and g) all the changes above combined (Simulation 6).

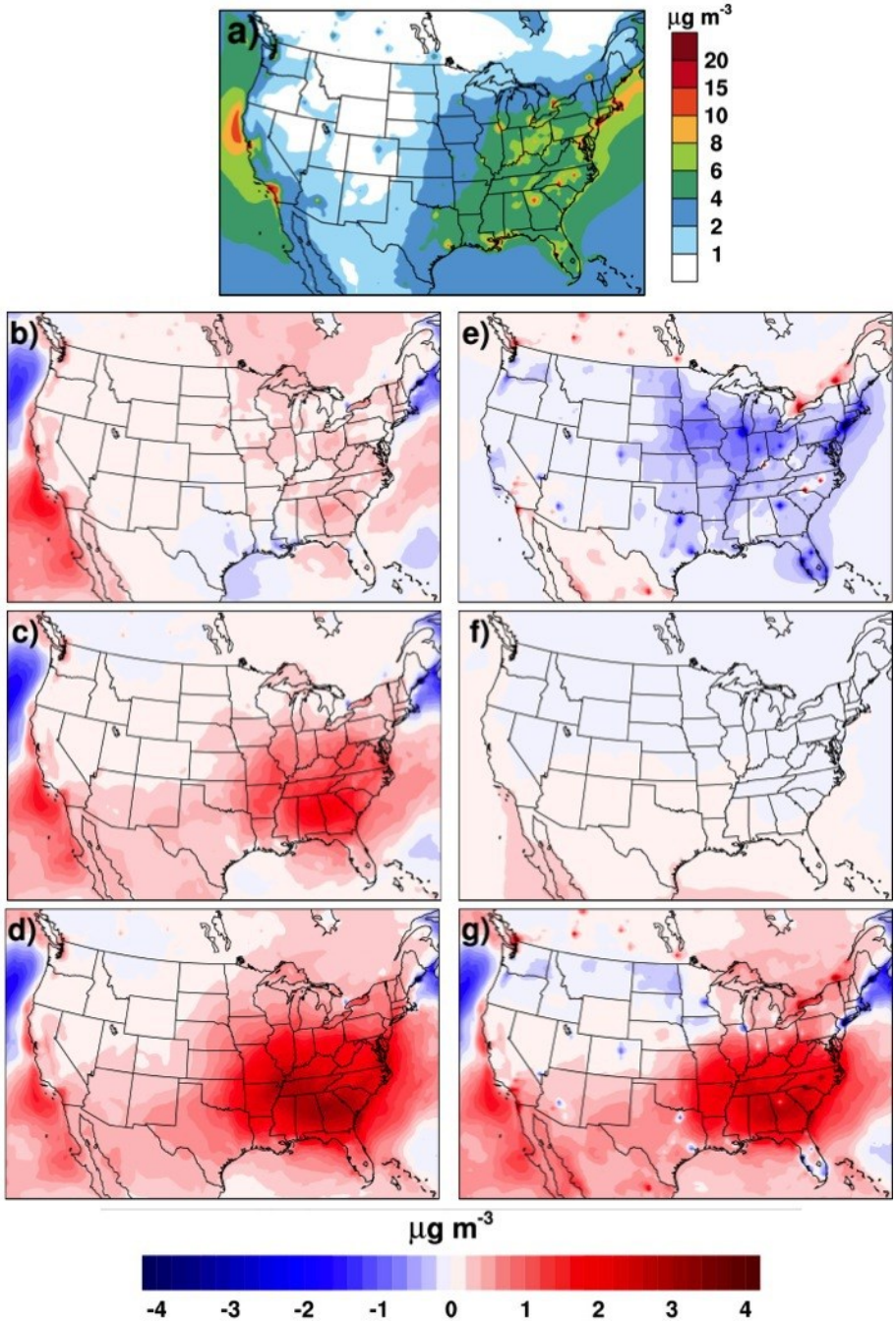

Figure 11. a) Current decade base case $PM_{2.5}$ average concentrations for five summers in the 2000s; spatial distribution and regional effect on $PM_{2.5}$ due to: b) changes in meteorology (Simulation 1); c) changes in meteorology and biogenic emissions (Simulation 2); d) changes in meteorology, biogenic emissions, and land use (Simulation 3); e) changes in US anthropogenic emissions (Simulation 4); f) changes in global anthropogenic emissions (Simulation 5); and g) all the changes above combined (Simulation 6).